Himalayan inverted metamorphism and syn-convergence extension as a consequence of a general shear extrusion

JEAN-CLAUDE VANNAY* & BERNHARD GRASEMANN‡

*Institut de Minéralogie et Pétrographie, Université de Lausanne, CH-1015 Lausanne, Switzerland
‡Institut für Geologie, Universität Wien, Althanstrasse 14, A-1090 Wien, Austria

(*Received* 13 April 2000; *revised version received* 21 November 2000; *accepted* 15 February 2001)

Abstract – Two paradoxical geological features of the Himalaya are the syn-convergence extension and the inverted metamorphic isograds observed in the crystalline core zone of this orogen. This High Himalayan Crystalline Sequence corresponds to an up to 40 km thick sequence of amphibolite to granulite facies gneiss, bounded by the Main Central Thrust at the base, and by the extensional faults of the South Tibetan Detachment System at the top. Geochronological and structural data demonstrate that coeval movements along both the Main Central Thrust and South Tibetan Detachment System during Early to Middle Miocene times were related to a tectonically controlled exhumation of these high-grade metamorphic rocks. The High Himalayan Crystalline Sequence systematically shows an inverted metamorphic zonation, generally characterized by a gradual superposition of garnet, staurolite, kyanite, sillimanite + muscovite and sillimanite + K-feldspar isograds, from the base to the top of the unit. Recent kinematic flow analyses of these metamorphic rocks demonstrate the coexistence of both simple shear and pure shear during the ductile deformation. The simple shear component of such a general non-coaxial flow could explain a rotation of isograds, eventually resulting in an inversion. The pure shear component of the flow implies a thinning of the metamorphic sequence that must be balanced by a perpendicular stretching of the unit parallel to its boundaries. Inasmuch as seismic data show that both the Main Central Thrust and South Tibetan Detachment System converge at depth, a thinning of the wedge-shaped High Himalayan Crystalline Sequence should induce a ductile extrusion of these high-grade rocks toward the surface. Rapid extension at the top of the sequence could thus be the consequence of a general shear extrusion of this unit relative to its hanging wall. Moreover, this extensional movement should decrease with depth to become zero where the boundaries of the unit meet, accounting for the paradoxical convergence of the South Tibetan Detachment System toward the Main Central Thrust. Furthermore, a general flow combining simple shear and pure shear can reconcile inverted isograds with the lack of inverted pressure field gradient across the High Himalayan Crystalline Sequence, despite an intense non-coaxial deformation. In good agreement with the seismic, kinematic and *P–T–t* constraints on the Himalayan tectono-thermal evolution, general shear extrusion provides a consistent model accounting for both inverted isograds and rapid extension in a compressional orogenic setting.

1. Introduction

Along the entire Himalayan belt, the crystalline core zone of this orogen consists of a 5 to 40 km thick metamorphic sequence, composed mainly of ductilely deformed, amphibolite to lower granulite facies paragneiss and minor granitic gneiss. Structural and seismic data indicate that this High Himalayan Crystalline Sequence corresponds to an orogenic wedge, bounded by the Main Central Thrust at its base, and by the extensional structures of the South Tibetan Detachment System at its top (Figs 1, 2a). Although the cause of such a significant synorogenic extension is still debated (e.g. Burchfiel & Royden, 1985; Chemenda *et al.* 1995; Grujic *et al.* 1996), geochronological constraints demonstrate that both the Main Central Thrust and South Tibetan Detachment System were active broadly contemporaneously during Early to Middle Miocene times (*c.* 20–15 Ma: e.g. Hodges *et al.* 1992; Hodges, Parrish & Searle, 1996; Dèzes *et al.* 1999, and references therein). These results indicate that the combined movements along these structures reflect a tectonic exhumation of the metamorphic core of the Himalayan orogen (for a comprehensive overview of the tectono-thermal evolution of the Himalaya–Tibet system, see Hodges, 2000).

An inverted metamorphic field gradient is almost systematically observed in sections across the High Himalayan Crystalline Sequence. From the Main Central Thrust to the top of the unit, this inverted metamorphic zonation is usually characterized by a gradual superposition of garnet, staurolite, kyanite, sillimanite + muscovite and sillimanite + K-feldspar isograds. An inverted metamorphism is also commonly observed in the units forming the footwall of the Main Central Thrust (e.g. Lesser Himalaya) and these rocks generally show a superposition of chlorite,

*Author for correspondence: Jean-Claude.Vannay@imp.unil.ch

https://doi.org/10.1017/S0016756801005313 Published online by Cambridge University Press

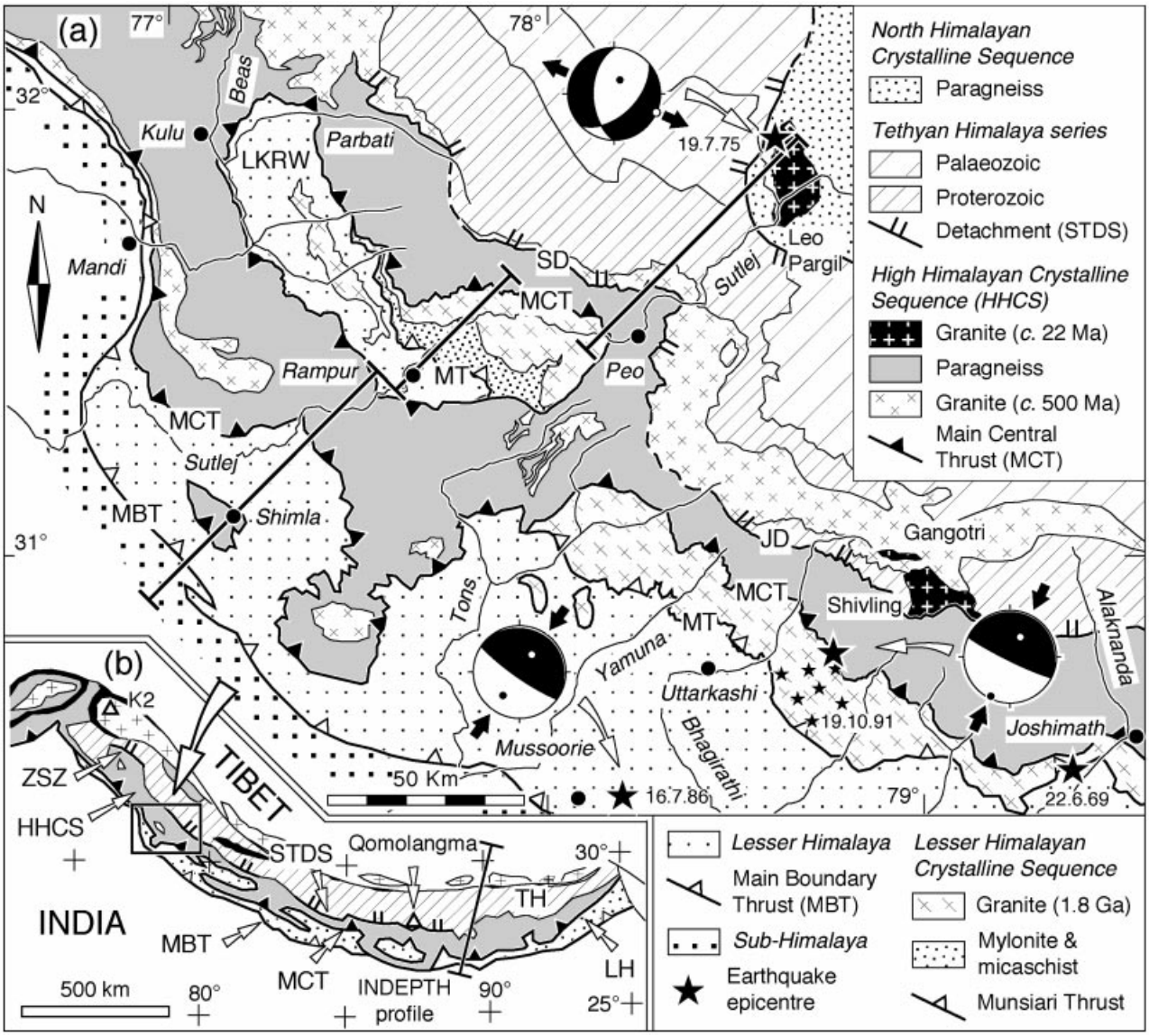


Figure 1. Geological context of the studied area. (a) Geological map of the Himachal Pradesh–Garhwal area in the Northwest Himalaya of India. Geology compiled after Jain & Anand (1988), Vannay & Grasemann (1998), Grasemann *et al.* (1999) and Searle *et al.* (1999a). Major earthquakes data for the illustrated area after Molnar & Lyon-Caen (1989) and Kayal (1996). Present-day seismic activity indicates that SW-directed thrusting occurs along the Main Boundary Thrust (MBT) and Munsiari Thrust (MT), in the footwall of the inactive Main Central Thrust (MCT), whereas WNW–ESE extension occurs in the Tethyan Himalaya, as a consequence of the E-directed lateral extrusion of Tibet (symbols for focal mechanism: black = contraction, arrow = orientation of shortening P axis). Other abbreviations: LKRW, Larji–Kulu–Rampur Window; SD, Sangla Detachment; JD, Jalha Detachment. (b) Generalized geological map of the Himalaya. Abbreviations: LH, Lesser Himalaya; MCT, Main Central Thrust; HHCS, High Himalayan Crystalline Sequence; STDS, South Tibetan Detachment System; ZSZ, Zanskar Shear Zone; TH, Tethyan Himalaya.

biotite and garnet zones. The inverted metamorphic field gradient is generally continuous across the Main Central Thrust in the internal parts of the orogen, but this continuity is often disrupted in the most frontal parts. Despite intensive efforts during the past decades to constrain the tectono-thermal evolution of the Himalayan orogen through quantitative approaches, its inverted metamorphism remains a debated issue. The parallelism between these inverted isograds and the Main Central Thrust at regional scale suggests a close genetic relation between inverted metamorphism and deformation during exhumation of the High Himalayan Crystalline Sequence (e.g. Pêcher, 1989). A major issue is whether the Himalayan inverted metamorphism reflects a syn-metamorphic inversion of isotherms during continental collision or the consequence of a late to post-metamorphic deformation of isograds through folding, shearing or thrusting. The

https://doi.org/10.1017/S0016756801005313 Published online by Cambridge University Press

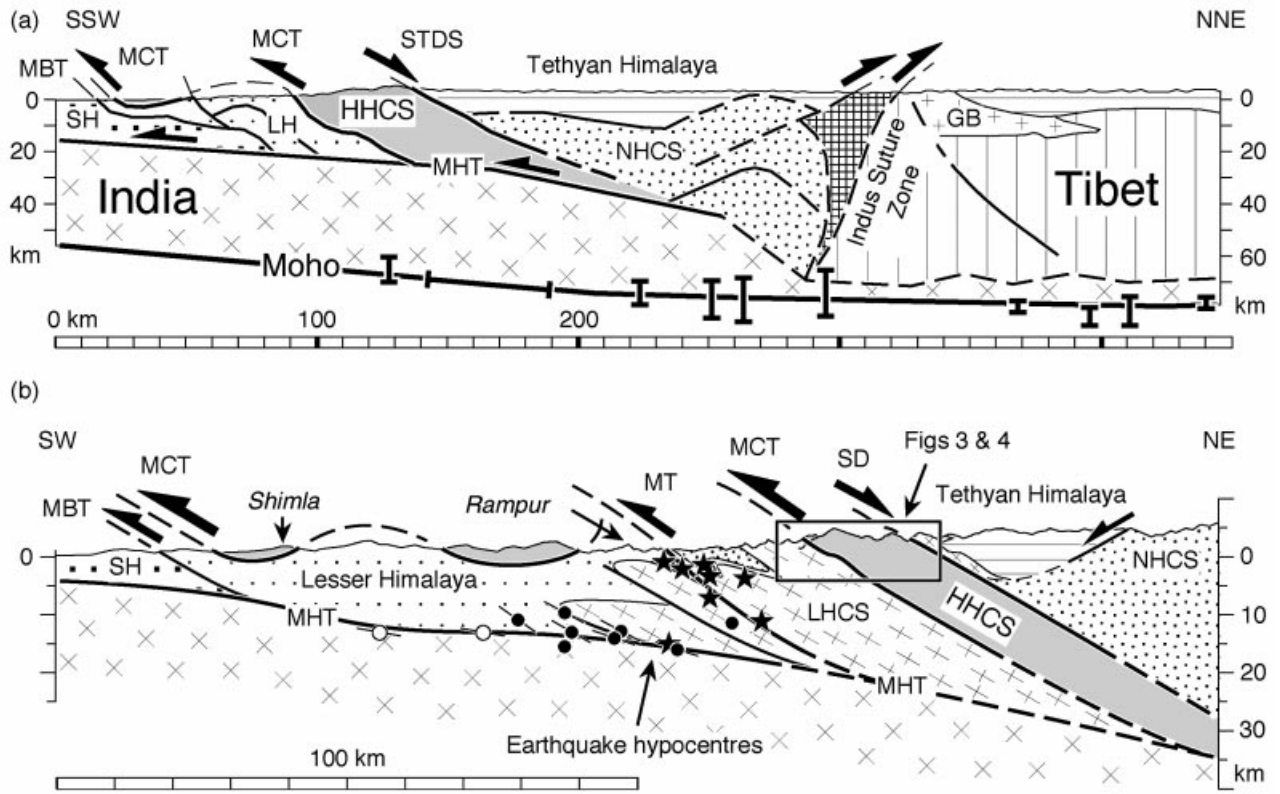


Figure 2. (a) General cross-section for the Southeast Himalaya at ~ 90° E (Fig. 1b), as constrained by the deep seismic reflection data of the International Deep Profiling of Tibet and the Himalaya project (INDEPTH, Hauck *et al.* 1998). Note the Main Central Thrust–Main Himalayan Thrust (MCT–MHT) and South Tibetan Detachment System (STDS) convergence at depth, and the gently dipping Moho beneath the Himalaya and South Tibet (sub-horizontal bar = reflection, vertical bars = receiver function analysis of earthquake data). (b) Geological cross-section for the Sutlej Valley, based on the geological map (Fig. 1), projected focal depth of earthquakes in this part of the Northwest Himalaya (black circles: Ni & Barazangi, 1984; white circles: Molnar & Lyon-Caen, 1989; stars: Kayal, 1996) and seismic data for the Main Himalayan Thrust beneath the Sub-Himalaya (Powers, Lillie & Yeats, 1998). Abbreviations: SH, Sub-Himalaya; LHCS, Lesser Himalayan Crystalline Sequence; NHCS, North Himalayan Crystalline Sequence; GB, Gangdese Batholith. Other abbreviations and symbols as in Figure 1.

aim of the present study is to summarize the main features of the Himalayan inverted metamorphism and syn-convergence extension, and to propose an alternative interpretation reconciling some paradoxical aspects of these phenomena. The ideas developed in the present study are based on new quantitative constraints on the tectonic and metamorphic evolution of the High Himalayan Crystalline Sequence in a typical Himalayan section. These results are summarized in the following section.

2. Sutlej section

The High Himalayan Crystalline Sequence is well exposed along the Sutlej Valley, in the Northwest Himalaya. Along the deep natural cross-section cut by this river across the High Himalayan range, this unit crops out as a 10 km thick, homogeneous sequence of high-grade pelitic paragneiss, dipping 30° to the northeast (Figs 1, 2b). This sequence is limited by the Main Central Thrust at its base, and by the extensional Sangla Detachment at its top. Toward the foreland, the Main Central Thrust becomes a shallow-dipping thrust, separating the High Himalayan Crystalline Sequence from the low- to medium-grade sediments of the Lesser Himalaya. The extent of the Main Central Thrust perpendicular to the range, from the northeastern limit of the Larji-Kulu-Rampur Window to the outermost klippe of High Himalayan Crystalline Sequence (Shimla Klippe), indicates a minimum displacement of about 100 km (Fig. 2b). Two phases of ductile deformation are observed in this unit. The dominant penetrative fabric in these rocks is the consequence of a D2 phase, associated with a SW-directed non-coaxial flow at the base and across most of the unit, and with NE-directed shearing at the top (Fig. 3). This D2 phase is interpreted to reflect the ductile stage of exhumation of the metamorphic sequence through combined thrusting along the Main Central Thrust and extension along the detachment at the top of the unit.

The High Himalayan Crystalline Sequence along the Sutlej traverse preserves an inverted metamorphic field

https://doi.org/10.1017/S0016756801005313 Published online by Cambridge University Press

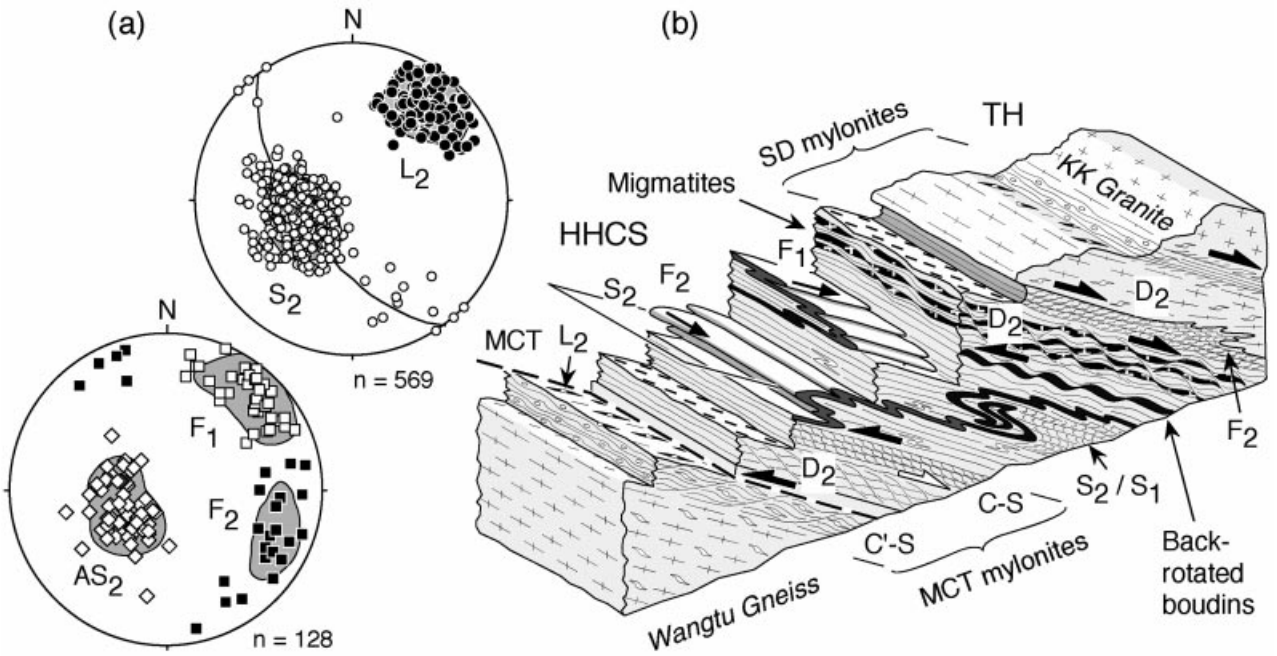


Figure 3. Ductile structures in the High Himalayan Crystalline Sequence along the upper Sutlej Valley. (a) Structural orientations projected in equal-area stereograms (lower hemisphere, shaded areas = five times random distribution). S = schistosity, L = mineral or stretching lineation, F = fold axis, AS = fold axial surface, KK Granite = Kinnaur Kailash Granite. Average orientation of the main penetrative fabrics: S_2 = 055/28 and L_2 = 038/24. (b) 'Ideal outcrop' block diagram summarizing the style and relations of the various structures (variable scale). The ductile non-coaxial deformation in the sequence is the consequence of two major phases, D_1 and D_2, responsible for the penetrative planar and linear fabrics. The relative chronology of these phases is revealed by fold interference patterns, as well as by a folded S_1 schistosity in the hinge zone of sub-isoclinal to tight F_2 folds. Larger amplitude, isoclinal F_1 folds have axial orientations parallel to the L_2 mineral lineation, suggesting a re-orientation of D_1 structures during the dominant D_2 phase. The D_1 phase is interpreted as being associated with the underthrusting of the High Himalayan Crystalline Sequence beneath the Tethyan Himalaya. The D_2 phase is associated with SW-directed thrusting along the Main Central Thrust (MCT) and NE-directed extension along the Sangla Detachment (SD) and it records the ductile stage of exhumation of the unit. Both the Main Central Thrust and Sangla Detachment are marked by mylonitic zones showing clear shear sense criteria (C–S fabrics, C'-type shear bands, sigma clasts and rotated blasts). Extensional C'-type shear bands superposed on the MCT D_2 mylonites mark the onset of a late phase of E- to ESE-directed extension.

gradient. In this unit, metamorphic conditions increase upwards from the staurolite zone at the base, through the kyanite-in and sillimanite-in isograds, to finally reach partial melting conditions at the top (Fig. 4). The absence of tectonic discontinuities within the sequence indicates that the upward increase in metamorphic grade is progressive. The metamorphic isograds are sub-parallel to the main schistosity and to the Main Central Thrust. The *P–T* conditions associated with this inverted metamorphism have been constrained by several methods (Fig. 4) and they consistently indicate peak conditions characterized by a temperature increase from $T \approx 570$ to 750 °C, at a nearly constant pressure around $P \approx 8$ kbar, from the base to the top of the sequence (Vannay & Grasemann, 1998; Vannay, Sharp & Grasemann, 1999). These results provide the first quantitative data confirming that the Himalayan inverted isograds can be associated with a complete inversion of the temperature field gradient across the metamorphic core of the orogen.

Together with a *P–T* path measured for the migmatitic paragneiss at the top of the unit, the peak *P–T* results strongly suggest the following tectonothermal evolution for the High Himalayan Crystalline Sequence in the Sutlej section (Fig. 5). (1) The almost constant peak pressure around 8 kbar indicates that peak conditions across the sequence were reached at a constant depth around 30 km. Moreover, the lack of pressure field gradient implies that no noticeable differential vertical movement of the samples, one relative to another, occurred during exhumation. In other words, the imaginary line connecting the samples collected across the sequence, the sampling line, did not rotate significantly with respect to the surface of Earth during exhumation from 30 km depth. (2) The inverted temperature field gradient associated with a constant depth indicates that the isotherms at the metamorphic peak were either dipping toward the foreland or inverted. (3) The calculated *P–T* path shows that peak conditions in the High Himalayan Crystalline Sequence were reached after a period of isobaric heating, indicative of a thermal relaxation

https://doi.org/10.1017/S0016756801005313 Published online by Cambridge University Press

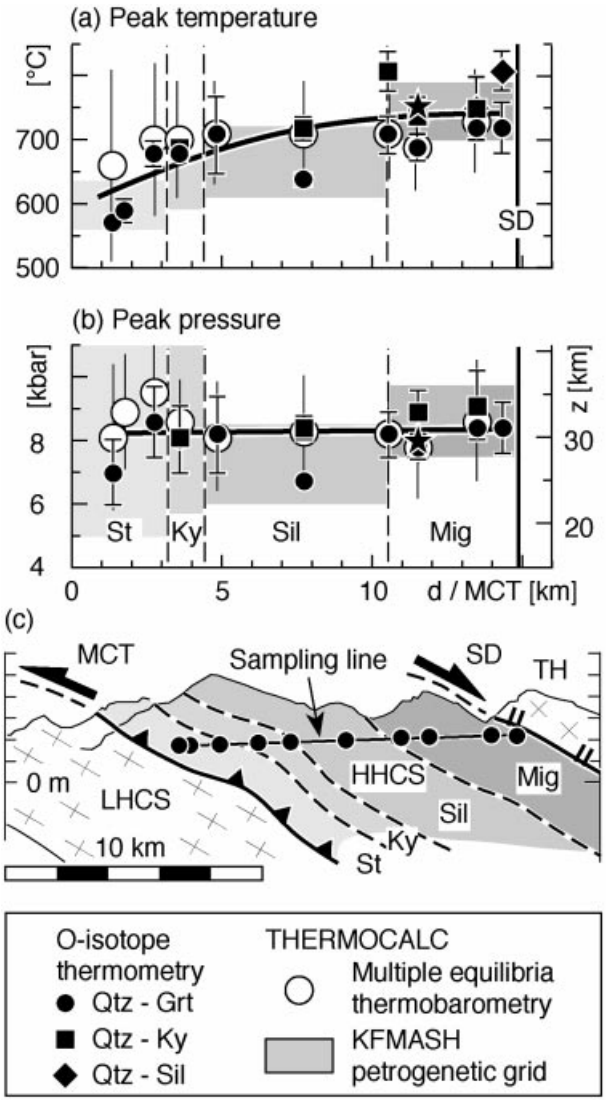


Figure 4. Temperature and pressure field gradients associated with inverted isograds in the High Himalayan Crystalline Sequence of the Sutlej section, after Vannay & Grasemann (1998) and Vannay, Sharp & Grasemann (1999). (a) Peak temperature determined by oxygen isotope thermometry on quartz (Qtz), garnet (Grt) and aluminosilicates pairs (Ky = kyanite, Sil = sillimanite), as well as by conventional, multiple equilibria, near-rim thermometry using THERMOCALC (Powell & Holland, 1994; Holland & Powell, 1998). (b) Peak pressure calculated by THERMOCALC for the measured temperatures. Symbols as in (a). Palaeodepth (z) based on a 0.27 kbar/km lithostatic gradient. The thick lines correspond to a curve and a linear fit for the *T* and *P* data, respectively. Error bars correspond to 2σ precision for isotopic thermometry and to 1σ accuracy for THERMOCALC results (Powell & Holland, 1994). Note that this latter accuracy overestimates significantly (5–10 times) the precision of the results (Worley & Powell, 2000). Shaded fields represent the *P–T* range for the stability of the diagnostic mineral assemblages in a K_2O-FeO-MgO-Al_2O_3-SiO_2-H_2O (KFMASH) petrogenetic grid calculated according to Holland & Powell (1998). The stars indicate *P–T* path peak conditions in the migmatites (Fig. 5c). (c) Geological setting (see Fig. 2b). The studied metapelites contain quartz+plagioclase+muscovite+biotite-bearing, low-Al assemblages, in which the gradual appearance of Barrovian index minerals reveals an inverted metamorphic zonation. Mineral zones: Grt = garnet, St = staurolite, Ky = kyanite, Sil = sillimanite + kyanite, Mig = sillimanite + kyanite-bearing migmatites. Black dots = analysed samples. Tectonic units and structures as in Figures 1 and 2.

after subduction (e.g. England & Thompson, 1984). Furthermore, the peak conditions were directly followed by cooling during decompression, and the retrograde *P–T* path remained close to the kyanite = sillimanite equilibrium (Fig. 5b). This retrograde evolution is consistent with the observed stability of both aluminosilicates in the sillimanite + kyanite-bearing samples, as well as with the complete lack of high-temperature/low-pressure assemblages, such as are observed in some other Himalayan sections (e.g. cordierite and/or andalusite-bearing assemblages; Brunel & Kienast, 1986; Dèzes *et al.* 1999). The *P–T* path thus implies a lack of significant thermal relaxation following onset of exhumation. Such a cooling along a more or less steady state geotherm most likely reflects the consequence of the cooling effect of both the footwall and hanging wall of the exhuming unit (Ernst & Peacock, 1996; Grasemann, Ratschbacher & Hacker, 1998). This *P–T* evolution is consistent with a tectonic extrusion of the High Himalayan Crystalline Sequence through combined thrusting at the base and extension at the top of the unit. In contrast, if the exhumation was controlled either by thrusting and erosion or by tectonic denudation and erosion, the metamorphic conditions at maximum depth (maximum pressure) should be followed by an initial phase of heating during decompression (clockwise *P–T* loop) or by isothermal decompression, respectively, as a consequence of heat advection during the initial stage of exhumation (e.g. England & Thompson, 1984).

The Middle Miocene to Early Pleistocene (16–1 Ma) exhumation and cooling of the High Himalayan Crystalline Sequence in the Sutlej Valley is constrained by $^{40}Ar/^{39}Ar$ muscovite ages and fission track ages (Jain *et al.* 2000; Grasemann, Vannay & Rahn, unpub. data). Such cooling is comparable to what is observed in the same unit in adjacent regions of the Northwest Himalaya, where peak conditions were reached between Late Oligocene and Early Miocene times, around 23 Ma (e.g. Dèzes *et al.* 1999, Searle *et al.* 1999*a*; Vance & Harris, 1999; Jain *et al.* 2000). About 70 km to the southeast of the Sutlej (Fig. 1), the Tertiary tectonothermal evolution of the High Himalayan Crystalline Sequence in the Bhagirathi section is well constrained by Sm–Nd (garnet–whole rock), U–Th–Pb (monazite), K–Ar and $^{40}Ar/^{39}Ar$ (biotite, muscovite and hornblende), and zircon and apatite fission track geochronology. These data suggest the following evolution: (1) Early to Late Oligocene (*c.* 35–25 Ma) pro-

https://doi.org/10.1017/S0016756801005313 Published online by Cambridge University Press

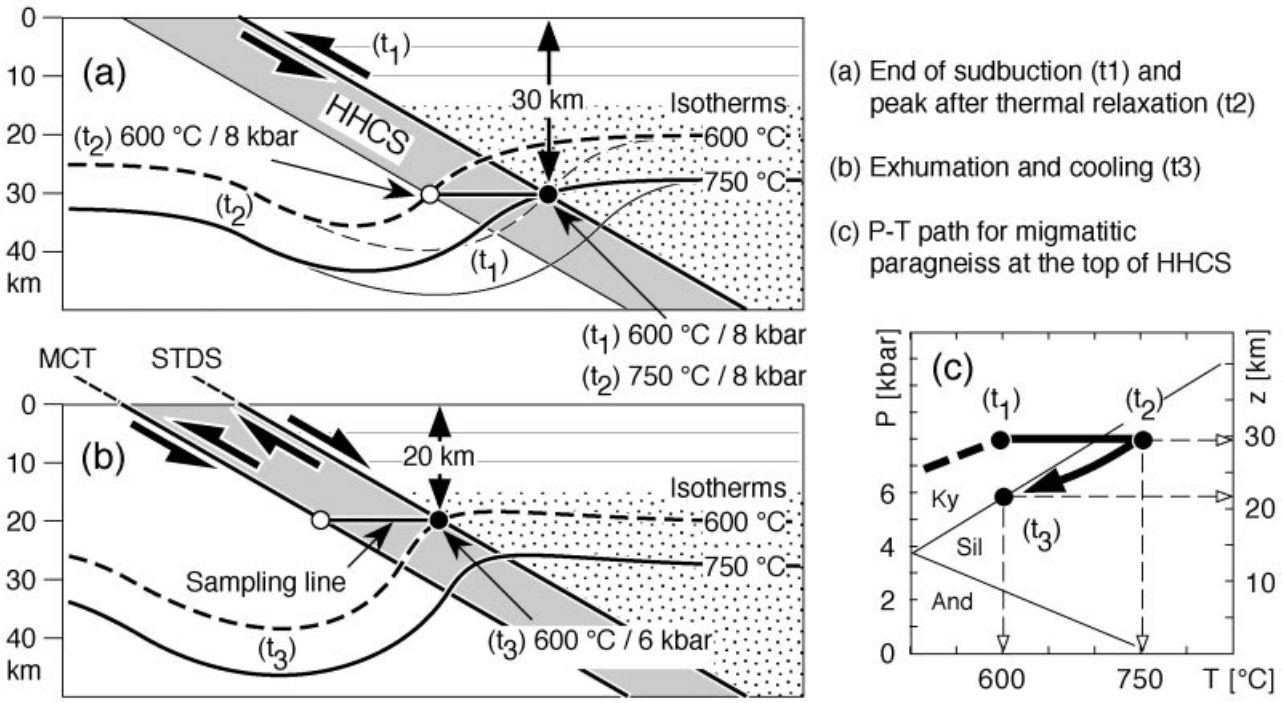


Figure 5. Tectono-thermal evolution of the High Himalayan Crystalline Sequence in the Sutlej section, based on *P–T* path and thermobarometry data (Fig. 4). (a) Subduction and prograde metamorphism. *P–T* path results indicate that the rocks at the top of the unit reached peak conditions after isobaric heating from *c.* 600 to 750 °C at 8 kbar, implying a period of thermal relaxation without significant tectonic activity. As a consequence, peak conditions along the sampling line across the sequence are reached at a nearly constant depth around 30 km. Temperatures increasing up-section along the sampling line at constant depth (Fig. 4) indicate that the isotherms at peak were at least dipping toward the foreland, although inverted isotherms cannot be ruled out. (b) Continuous cooling during decompression and exhumation of the High Himalayan Crystalline Sequence (HHCS) indicates a tectonic extrusion of the unit as a result of coeval movements along the Main Central Thrust (MCT) and South Tibetan Detachment System (STDS). Note that the thermal structure illustrated corresponds to isotherms during cooling and not peak isograds (see text for discussion). (c) *P–T* path for the migmatitic paragneiss at the top of the High Himalayan Crystalline Sequence, determined by thermodynamic modelling (Vannay & Grasemann, 1998); And = andalusite.

grade metamorphism up to upper amphibolite facies; (2) Late Oligocene to Early Miocene metamorphic peak and partial melting around 23 Ma; (3) Early Miocene rapid cooling, associated with ductile thrusting along the Main Central Thrust and extension along the South Tibetan Detachment System, between 23 and 20 Ma; and (4) Middle Miocene to Late Pliocene (*c.* 15–2 Ma) slow cooling, controlled by erosion and thrusting in the footwall of the Main Central Thrust up to 5.7 Ma (Metcalfe, 1993; Prince *et al.* 1994; Sorkhabi *et al.* 1996; Catlos *et al.* 1999; Searle *et al.* 1999*a*). Given the lateral continuity of the High Himalayan Crystalline Sequence between the Bhagirathi and the Sutlej sections (Fig. 1, Jain & Anand, 1988), the similar structural setting (Metcalfe, 1993; Vannay & Grasemann, 1998), and the comparable Middle Miocene to Late Pliocene cooling histories, it is likely that this sequence in the Sutlej Valley also experienced an Early Miocene metamorphic peak followed by a rapid exhumation. In the Sub-Himalayan foreland basin near Shimla, at the south-western end of the studied section (Figs 1, 2b), Najman & Garzanti (2000) observed that the Early Miocene Kasauli Formation records a sudden influx of detrital garnet beginning at *c.* 22 Ma. According to these authors, this observation implies an abrupt unroofing of metamorphic rocks that is not compatible with a gradual erosion, and it supports a tectonically controlled exhumation of the High Himalayan Crystalline Sequence in this part of the Northwest Himalaya during Early Miocene times.

3. Himalayan inverted metamorphism

Although known for more than a century (e.g. Mallet, 1875), the Himalayan inverted metamorphism is one of the most puzzling and debated geological features on Earth. The contrasted models proposed to explain this inverted metamorphism may partly reflect along-strike variations in the Himalayan tectono-metamorphic evolution, but the fact that inverted isograds are observed for more than 1700 km along the belt suggests that some first-order process must control this phenomenon. Consequently, the debate about the cause of the inverted metamorphism raises some fundamental questions about the tectono-thermal evolution of the Himalayan orogen.

https://doi.org/10.1017/S0016756801005313 Published online by Cambridge University Press

3.a. Does the Himalayan inverted metamorphism reflect inverted isotherms?

Several thermal models propose an inversion of isotherms controlled by heat production, conduction and/or advection processes in the crust during the Himalayan orogeny. The so-called 'hot iron' model, for example, invokes a syn-thrusting, transient inversion of the isotherms at the level of the Main Central Thrust, as a result of downward heat conduction between the hot, exhuming hanging wall (High Himalayan Crystalline Sequence) and the colder footwall of the thrust (Frank *et al.* 1973; LeFort, 1975). This qualitative model predicts that, as a consequence of a retrograde metamorphic evolution in the hanging wall of the Main Central Thrust, the temperature should increase upwards across the thrust zone, to reach a maximum at some structural level within the hanging wall, to subsequently decrease upwards. Such features are not consistent with the lack of significant retrograde metamorphism in the hanging wall of the thrust in the internal parts of the orogen, as well as with the continuous increase in peak temperature from the base to the top of the High Himalayan Crystalline Sequence in the Sutlej section (Fig. 4). More generally, this model implies a complete resetting of the metamorphic assemblages by retrograde, net-transfer reactions in most of the hanging wall of the Main Central Thrust. Such a systematic re-equilibration is neither consistent with the exponential decrease of reaction rates during cooling, nor with the necessity for water to be pervasively available for most of these retrograde hydration reactions to proceed. In contrast, oxygen isotope results for the Sutlej section indicate that most of the High Himalayan Crystalline Sequence rocks behaved as closed, anhydrous systems during the metamorphic peak and the subsequent cooling (Vannay, Sharp & Grasemann, 1999). Consequently, although the 'hot iron' model could account for prograde inverted isotherms and isograds in the footwall of the Main Central Thrust, it is not consistent with the preservation of metamorphic peak assemblages in its hanging wall.

In order to account for the metamorphic features of the High Himalayan Crystalline Sequence rocks now exposed at the surface, notably the dehydration melting conditions of metapelites constrained by thermobarometry results (e.g. Dèzes *et al.* 1999; Vannay, Sharp & Grasemann, 1999), a thermal model should be able to predict inverted isotherms sub-parallel to the Main Central Thrust and peak temperatures in excess of 700 °C at about 30 km depth (LeFort, 1975). Given the still large uncertainty in the parameters controlling the thermal evolution of an orogen, the conclusions drawn from the numerous quantitative thermal models for the Himalaya vary significantly. For a reasonable convergence rate of 2 cm/yr along the Main Central Thrust, one- and two-dimensional numerical thermal models predict, however, that the 'hot iron' effect alone cannot induce inverted isotherms at 30 km depth (e.g. Shi & Wang, 1987). Two-dimensional thermal models further confirm that a thermal inversion at depths greater than 20 km would not occur even if the thrusting rate is increased to the unlikely value of 5 cm/yr, and if the contrast in thermal conductivity between the metamorphic rocks and the overlying sedimentary series of the Tethyan Himalaya ('heat focussing': Jaupart & Provost, 1985) is taken into account (Grasemann, 1993). Shear heating at the level of the Main Central Thrust (e.g. England & Molnar, 1993; Harrison *et al.* 1998) can potentially induce an inverted geotherm in the footwall of the thrust, but not in its hanging wall. Moreover, such a process predicts maximum temperatures near the Main Central Thrust, in contrast to the temperature field gradient measured for the Sutlej and several other Himalayan sections (Fig. 4; e.g. Hodges, LeFort & Pêcher, 1988; Jain & Manickavasagam, 1993; MacFarlane, 1995; Searle *et al.* 1999*b*). A third type of thermal model, combining the effects of accretion of crustal material enriched in heat-producing elements and erosion-controlled heat advection, has also been invoked to explain inverted isotherms (Royden, 1993; Huerta, Royden & Hodges, 1996). Such thermal models are, however, highly time-dependent as radiogenic heat production and erosion are relatively slow processes. Although they must enhance the geothermal gradient in the thickened crust, it is not clear whether these processes alone could have induced inverted isotherms in the High Himalayan Crystalline Sequence during the *c.* 30 m.y. time interval between the onset of collision and activation of the Main Central Thrust. For example, the 2-D thermal model by Huerta, Royden & Hodges (1996) predicts that maximum temperatures above 600 °C around 30 km depth are reached after *c.* 30 m.y., and that more than 100 m.y. are required to reach temperatures in excess of 700 °C. Consequently, although quantitative thermal models predict that isotherms are readily bent toward the foreland during continental underthrusting, these isotherms are not necessarily inverted as easily as suggested by the qualitative 'hot iron' model.

3.b. Does the Himalayan inverted metamorphism reflect deformed isograds?

Emphasizing the intense ductile non-coaxial deformation observed throughout the High Himalayan Crystalline Sequence, several models interpret the Himalayan inverted metamorphism as the consequence of a late to post-metamorphic deformation of isograds. The earliest interpretation proposed an inversion of isograds by large-scale recumbent folding (von Loczy, 1907 *in* Gansser, 1964; Searle *et al.* 1999*b*), yet such large-scale folds have been identified in only a few Himalayan sections (e.g. Frank *et al.* 1973), and inverted isograds are also observed in units proved to

https://doi.org/10.1017/S0016756801005313 Published online by Cambridge University Press

have a normal structural polarity (e.g. Gansser, 1964). An inversion of isograds through ductile simple shear (Thöni, 1977; Jain & Manickavasagam, 1993; Grujic *et al.* 1996; Hubbard, 1996; Grasemann & Vannay, 1999), or by tectonic imbrication along thrusts (Treloar *et al.* 1989; Swapp & Hollister, 1991), does not require an inversion of the rock sequence. Although ductile non-coaxial deformation is ubiquitous, post-metamorphic thrusts within the High Himalayan Crystalline Sequence have only rarely been described, however, and such structures have not been observed in the Sutlej section.

Because the above-mentioned kinematic models propose that the inverted metamorphism reflects a deformation-controlled superposition of deeper, higher-grade rocks onto shallower, lower-grade rocks, they predict that inverted isograds should be associated with a significantly inverted pressure field gradient. In contrast, most of the quantitative *P–T* data for the High Himalayan Crystalline Sequence, including those for the Sutlej section, indicate either a gradual up-section decrease in peak pressure or a nearly constant peak pressure across the sequence, from northwestern India to Bhutan (e.g. Brunel & Kienast, 1986; Hodges, LeFort & Pêcher, 1988; Hodges & Silverberg, 1988; Hubbard, 1989; Pêcher, 1989; MacFarlane, 1995; Rai *et al.* 1998; Searle *et al.* 1999*b*; Vannay, Sharp & Grasemann, 1999; Fraser, Worley & Sandiford, 2000).

3.c. Do inverted isograds reflect combined thermal and tectonic processes?

Thermal models focused on the thermal evolution of units modelled as undeforming plates ignore the potential influence of the ductile deformation that is systematically observed across the High Himalayan Crystalline Sequence. A fully coupled thermal–mechanical model by Jamieson *et al.* (1996) suggests that the interaction between ductile flow and thermal evolution during an orogeny could lead to inverted isograds without requiring inverted isotherms at the metamorphic peak. The main limitation of this large-scale 'numerical orogen' model is that it considers the Main Central Thrust as a 'retroshear', dipping in the opposite direction to the modelled S-directed continental subduction, in contrast to structural and geophysical results confirming a northward subduction of India beneath Asia. This model has, however, the major merit of emphasizing the interdependence of the thermal evolution and the ductile deformation during an orogeny.

4. Himalayan syn-convergence extension

Although synorogenic extensional shear zones at the top of the High Himalayan Crystalline Sequence are a recent discovery (Burg *et al.* 1984), they have been described in numerous sections all along the range (Herren, 1987; Burchfiel *et al.* 1992; Dèzes *et al.* 1999, and references therein). Unlike the Main Central Thrust, these extensional structures are not continuous along the strike of the orogen, and they are generally referred to as the South Tibetan Detachment System (STDS; Burchfiel *et al.* 1992). Geochronological data indicate that these structures have been active mainly during Early Miocene times (22–16 Ma), but movements younger than 12.5 Ma have also been determined (Hodges *et al.* 1992, 1998; Hodges, Parrish & Searle, 1996; Edwards & Harrison, 1997; Coleman, 1998; Dèzes *et al.* 1999; Hodges, 2000). Quantitative constraints on minimum slip are available for two strands of the South Tibetan Detachment System, about 1000 km apart. In Nepal, a minimum displacement of 35 km occurred along the Qomolangma Detachment between 22 and 16 Ma (Burchfiel *et al.* 1992; Hodges *et al.* 1992, 1998). In Zanskar, the 150 km long Zanskar Shear Zone accommodated a minimum ductile slip of 35 km between approximately 23 and 20 Ma (Herren, 1987; Dèzes *et al.* 1999; Vance & Harris, 1999). Ductile shearing along the Main Central Thrust zone initiated *c.* 22 Ma, and deformation associated with prograde metamorphism in the footwall of this thrust lasted at least until *c.* 6 Ma in some areas (e.g. Hubbard & Harrison, 1989; Hodges, Parrish & Searle, 1996; Coleman, 1998; Catlos *et al.* 1999). The South Tibetan Detachment System and Main Central Thrust thus appear to have been broadly contemporaneous for probably 10 m.y. These combined movements could have been episodic and not necessarily synchronous, but they were most likely related to a rapid, tectonically controlled exhumation of the Himalayan metamorphic core, at least from the Northwest Himalaya to Nepal (e.g. Hodges, Parrish & Searle, 1996; Wyss, Hermann & Steck, 1999).

Seismic data show that both the Main Central Thrust and South Tibetan Detachment System converge at depth, defining an orogenic wedge (Fig. 2a, Hauck *et al.* 1998). As both these structures were activated around 22 Ma, the convergence of these two major shear zones delimiting the High Himalayan Crystalline Sequence is most likely a primary feature that already existed at the onset of exhumation. Continuous thrusting and continental accretion in the footwall of the Main Central Thrust (e.g. Main Boundary Thrust) probably induced some tilting of the High Himalayan Crystalline Sequence, but such movements could not have modified significantly the overall wedge geometry of the unit. Consequently, this sequence is considered as an orogenic wedge exhumed during Early Miocene times in most current models for the Himalaya (e.g. Chemenda *et al.* 1995; Grujic *et al.* 1996; Hodges, Parrish & Searle, 1996; Chemenda, Burg & Mattauer, 2000). As reviewed by Platt (1993), the overall geometry of an orogenic wedge can significantly affect its exhumation mechanism.

https://doi.org/10.1017/S0016756801005313 Published online by Cambridge University Press

4.a. Gravitational collapse

It has been proposed that the South Tibetan Detachment System is the result of the gravitational collapse of a Miocene topographic front between India and Tibet. Treating the Indo-Tibetan lithosphere as a perfectly elastic half-space under horizontal compression, Burchfiel & Royden (1985) showed that an abrupt change in elevation can theoretically induce a field of sub-horizontal minimum effective stress in the contracting orogen. For a topographic gradient comparable to the present-day profile, and increasing from zero to 5 km between the Indian shield and the Tibetan plateau, such a minimum effective stress field could extend for several tens of kilometres north of the topographic front, and induce extension down to 10–20 km depth. Seismic data show that the South Tibetan Detachment System at 90° E longitude can be followed down to a current depth of at least 15 km. According to Hauck *et al.* (1998), this detachment appears to continue down to about 30 km depth, possibly merging with the Main Central Thrust–Main Himalayan Thrust (Fig. 2a). Moreover, the original maximum depth reached by the detachment was certainly greater, given the significant erosion of the Himalaya since Early Miocene times. Considering the average denudation rate of 1 km/m.y. for the High Himalayan range during the past 20 m.y., as calculated by Einsele, Ratschbacher & Wetzel (1996), the original depth reached by the South Tibetan Detachment System could have been up to 50 km. Furthermore, the isostatic surface elevation of Tibet during Early Miocene times was most likely in the order of only 2 km, and a major surface uplift of Tibet to its current height (5 km) is considered to be a later process, probably occurring after *c.* 8 Ma (e.g. Fielding, 1996). Consequently, a topographically controlled gravitational collapse should have been confined to shallow crustal levels in the Himalaya, and it is not clear that such a process could have affected the deep crustal levels of an orogen contracting at 1 to 2 cm/yr (Bilham *et al.* 1997; Powers, Lillie & Yeats, 1998).

4.b. Buoyancy-controlled crustal exhumation

On the basis of analogue experiments, Chemenda *et al.* (1995) proposed that both the Main Central Thrust and South Tibetan Detachment System reflect the exhumation movement of the High Himalayan Crystalline Sequence as the consequence of buoyancy forces counteracting the subduction of 'light' continental crustal rocks. This model predicts that following subduction of the entire Indian lithosphere down to 200–300 km depth, the upper crust starts to decouple from the sub-crustal lithosphere and to exhume by buoyancy. Compared to the significant subduction depth simulated by this model, the movement along the South Tibetan Detachment System is constrained to be between 30 and 100 km (Burchfiel *et al.* 1992; Hauck *et al.* 1998; Dèzes *et al.* 1999). Consequently, this model predicts that a significant 'root' of crustal rocks should still be dipping in the asthenosphere (e.g. fig. 5 in Chemenda *et al.* 1995), and that the Moho beneath the Himalaya should reach about 100–270 km depth. Although recent tomographic results confirm that the Indian continental lithosphere is subducted down to 1000 km beneath some parts of the Himalaya (Van der Voo, Spakman & Bijwaard, 1999), seismic results from the INDEPTH project indicate a gently dipping Moho between 55 to 75 km beneath the Himalaya and south Tibetan plateau (Fig. 2a). This suggests that decoupling of the Indian crust from the lithosphere during subduction could have taken place earlier than suggested by the model of Chemenda *et al.* (1995), and that the crust has not been necessarily subducted to great depths during the collision (Hauck *et al.* 1998).

This point emphasizes that a buoyancy-controlled crustal exhumation is highly dependent on the rheology of the weak lower crust, that controls the coupling between the light upper crust and the denser sub-crustal lithosphere, yet variations of rheology as a function of the temperature increase during subduction are not simulated in the purely mechanical experiments by Chemenda *et al.* (1995). This point has been addressed in new thermo-mechanical modelling by Chemenda, Burg & Mattauer (2000), suggesting that the evolution of the Himalaya–Tibet system could have involved underplating beneath Tibet either of the entire Indian lithosphere or of the Indian upper crust delaminated from the sinking sub-crustal lithosphere. These thermo-mechanical experiments do not simulate, and are incompatible with, the deep subduction and subsequent buoyancy-controlled exhumation of the upper crust, such as observed in the purely mechanical experiments by Chemenda *et al.* (1995). Additionally, the models by Chemenda *et al.* (1995) and Chemenda, Burg & Mattauer (2000) do not account for the fact that the High Himalayan Crystalline Sequence consists predominantly of paragneiss representing essentially the metamorphosed sedimentary cover of the Indian plate, and not the entire upper crust (Fig. 2a, e.g. Gansser, 1964; Brunel & Kienast, 1986; Hodges & Silverberg, 1988; Hubbard, 1989; Pêcher, 1989; MacFarlane, 1995; Vannay & Hodges, 1996; Searle *et al.* 1999*b*, Vannay & Grasemann 1998).

4.c. Channel flow ductile extrusion

Along the entire Himalayan belt, the rocks of the High Himalayan Crystalline Sequence are pervasively deformed by non-coaxial shearing (e.g. Gansser, 1964; Brunel & Kienast, 1986; Jain & Manickavasagam, 1993; Metcalfe, 1993; Hodges, Parrish & Searle, 1996; Vannay & Hodges, 1996; Wyss, Herman & Steck, 1999). On the basis of an analysis of quartz

https://doi.org/10.1017/S0016756801005313 Published online by Cambridge University Press

microfabric from this unit in Bhutan, Grujic *et al.* (1996) demonstrated the coexistence of both simple shear and pure shear, in other words a general non-coaxial flow, during the ductile deformation of these rocks. These authors thus proposed a qualitative kinematic channel flow model, considering the High Himalayan Crystalline Sequence as a wedge of hot metamorphic rocks, deformed ductilely between colder and more rigid rocks of the underthrusting plate (Main Central Thrust footwall) and a backstop formed by the South Tibetan Detachment System hanging wall (Tethyan Himalaya). In this model, pure shear deformation related to an induced lateral pressure gradient produces a 'pipe-flow', characterized by the highest velocities in the centre of the channel, and by opposite simple shear movements in the upper and lower parts of the unit. Such a heterogeneous simple shear could lead to an extrusive flow in the wedge-shaped unit, contributing to exhumation and to shear isograds. Grujic *et al.* (1996) proposed that this extrusive flow could be the consequence of an orogen-perpendicular pressure gradient *c.* 1–2 kbar/km, induced by a topographic gradient of 4–6 km over a horizontal distance about 100 km. It is not clear, however, whether such a strong topographic gradient, similar to the present-day one, already existed before exhumation of the High Himalayan Crystalline Sequence during Early Miocene times, because the elevation of Tibet at that time was most likely only about 2 km (e.g. Fielding, 1996). Moreover, the fact that the High Himalayan Crystalline Sequence forms the core of the High Himalayan range suggests that the exhumation of this sequence is more likely to be the cause, rather than the consequence, of the present-day topographic gradient across the Himalaya. On the basis of new structural investigations, Grasemann, Fritz & Vannay (1999) suggested that the top and bottom shear zones of the High Himalayan Crystalline Sequence wedge deformed by general shear and, due to the requirements of strain compatibility, the centre of the wedge extruded mainly as a consequence of the pure shear component of the flow, in contrast to the heterogeneous simple shear invoked by Grujic *et al.* (1996). A ductile extrusion of the High Himalayan Crystalline Sequence, either heterogeneous or homogeneous, is consistent with the fact that seismic data indicate that this unit is a wedge, bounded by two tectonic contacts (Main Central Thrust and South Tibetan Detachment System) converging at depth (Fig. 2a).

5. Material lines and non-coaxial flow

A major limitation of the kinematic models proposing an inversion of isograds by ductile shearing (Thöni, 1977; Jain & Manickavasagam, 1993; Grujic *et al.* 1996; Hubbard, 1996; Grasemann & Vannay, 1999) is that they do not consider the implications of a non-coaxial flow on the pressure field gradient across the High Himalayan Crystalline Sequence. With reference to the structural and *P–T* results for the Sutlej section (Figs 3, 4, 5), the inverted isograds issue discussed above can be summarized by the following question. Is it possible to reconcile inverted isograds in the High Himalayan Crystalline Sequence with: (1) a lack of inverted pressure field gradient; (2) the ductile non-coaxial deformation systematically observed across the entire metamorphic sequence; and (3) the predictions of quantitative thermal models suggesting that peak isotherms are readily bent toward the foreland, but not necessarily inverted, during a continental collision?

5.a. Isograds and sampling profile as material lines

The *P–T* results for the High Himalayan Crystalline Sequence in the Sutlej section indicate that the peak temperatures across the unit were reached at a nearly constant depth, as a consequence of a thermal relaxation after subduction (Fig. 5a,b). During post-peak cooling and deformation (Fig. 5c), isograds can be used as an approximation of 'palaeoisotherms' at peak, if the first appearance of an index mineral is mainly controlled by the temperature (Grasemann & Vannay, 1999). Most of the isograd reactions of a Barrovian metamorphic field gradient in metapelites, such as the discontinuous staurolite-in or kyanite-in reactions observed in the High Himalayan Crystalline Sequence, are characterized by steep d*P*/d*T* slopes in a petrogenetic grid, implying that they are mainly temperature-controlled. For example, the temperature difference between 20 and 40 km depth for the staurolite-in and kyanite-in reactions is *c.* 65 and 45 °C, respectively, in a K_2O-FeO-MgO-Al_2O_3-SiO_2-H_2O (KFMASH) petrogenetic grid calculated according to Holland & Powell (1998). Consequently, such isograds represent fairly close approximations of palaeoisotherms at peak within the High Himalayan Crystalline Sequence, as it is generally assumed by the thermal models for the inverted metamorphism. During exhumation and cooling, these isograds can be considered as material lines, acting as passive markers during deformation. Another such material line is the one that connected during peak conditions at depth the samples that can now be collected across the exhumed metamorphic sequence (Fig. 6a). The lack of pressure field gradient across the High Himalayan Crystalline Sequence of the Sutlej section (Fig. 4) indicates that this sampling line was already sub-horizontal at peak, and that it did not rotate significantly during the subsequent exhumation.

5.b. Eigenvectors of the flow

During ductile deformation, the sense and rate of rotation of material lines is strongly dependent on the type of flow, as well as on their initial orientation

https://doi.org/10.1017/S0016756801005313 Published online by Cambridge University Press

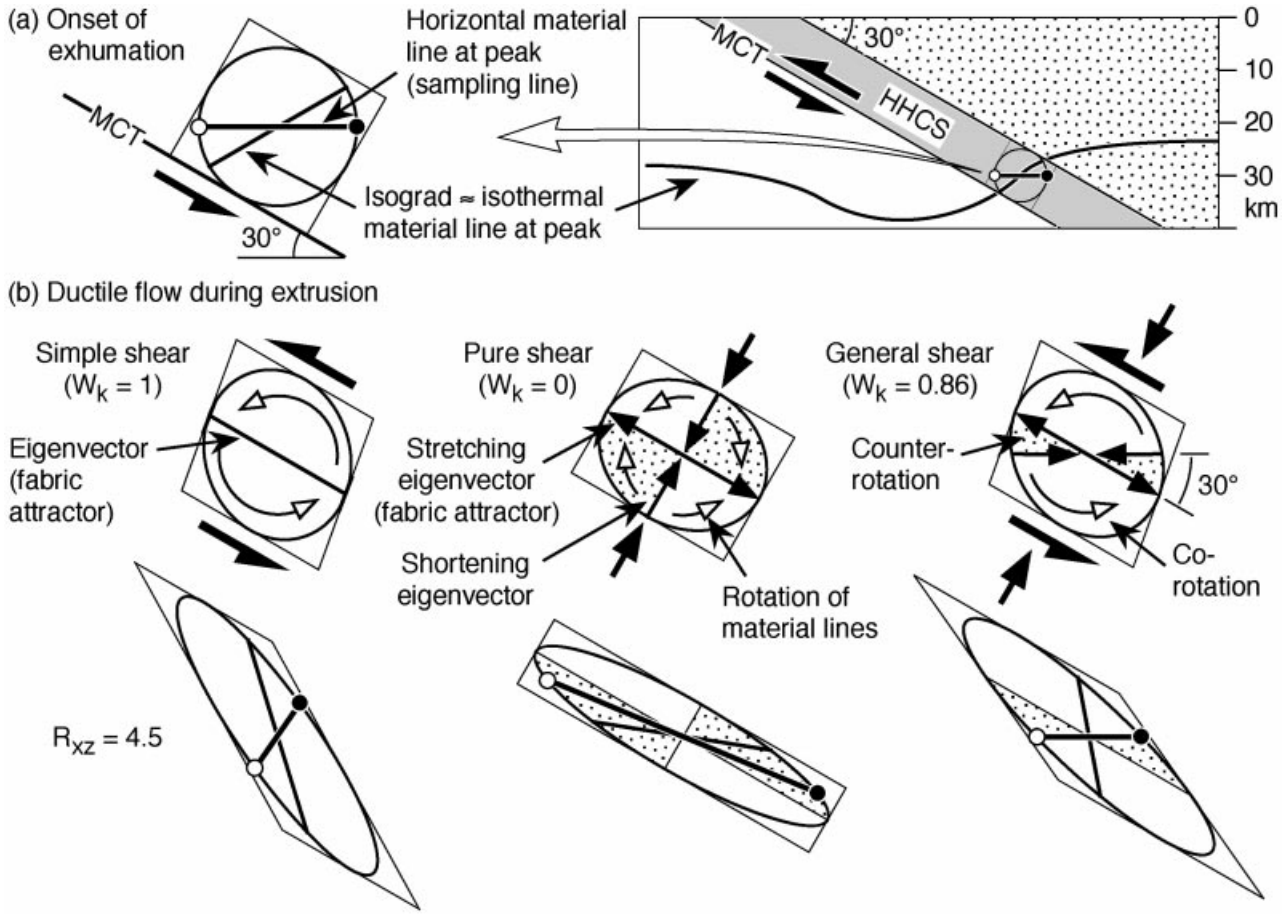


Figure 6. Material lines and ductile shear flow. (a) Metamorphic peak and onset of exhumation of the High Himalayan Crystalline Sequence (HHCS). *P–T* data (Fig. 4) indicate that the sampling line (imaginary material line connecting the samples collected across the exhumed sequence) was parallel to Earth's surface at 30 km depth, and that the isotherms at peak were at least dipping toward the foreland (Fig. 5). These isotherms become passive isograds during exhumation and cooling. (b) Rotation of material lines for three types of ductile shear flow (isochoric plane strain flow). The eigenvectors represent the irrotational directions of the flow. The cosine of the angle between the eigenvectors of the flow corresponds to the kinematic vorticity number W_k. Because it implies that the sampling line remained parallel to Earth's surface during exhumation, the lack of pressure field gradient across the High Himalayan Crystalline Sequence (Fig. 4) is compatible only with a general non-coaxial flow (simple + pure shear). The present-day dip of the unit (*c.* 30°) suggests a ductile extrusion through a general flow characterized by a mean kinematic vorticity number $W_m \approx 0.86$ (= cosine of 30°; see text for discussion).

(Ramberg, 1975). As a first-order approximation, the High Himalayan Crystalline Sequence can be considered as a thick, ductile shear zone, bounded by the Main Central Thrust and South Tibetan Detachment System (Figs 2, 3; Grujic *et al.* 1996). The relations between different types of homogeneous ductile flow and the rotation of a horizontal sampling line and a foreland-dipping isograd at peak (Fig. 5) are illustrated in Figure 6. The geometry of the flow is conveniently described by the nature and orientation of the eigenvectors of the flow tensor, that have the characteristics that lines parallel to these directions will not rotate during deformation (Ramberg, 1975).

Ideal simple shear is characterized by only one eigenvector, parallel to the shear zone boundaries. Ideal pure shear is characterized by a stretching eigenvector parallel to the shear zone boundaries, and a perpendicular shortening eigenvector. During deformation, material lines oblique to the eigenvector(s) of the flow rotate toward the irrotational direction parallel to the shear zone boundaries. Consequently, this latter eigenvector acts as a 'fabric attractor' (Passchier & Trouw, 1996), which orientation is approximated in ductile rocks by a penetrative foliation, whereas a penetrative lineation reflects the direction of the flow. The sense of rotation of the material lines depends on their initial orientation with respect to the eigenvectors. For the setting illustrated in Figure 6, the isograd and the horizontal sampling line at peak can rotate either toward the foreland or toward the hinterland, as a function of the type of flow. In the High Himalayan Crystalline Sequence, the orientation of the fabric attractor of the ductile flow is approximated by the penetrative S2 schistosity, that is sub-parallel to the Main Central Thrust (Fig. 3).

https://doi.org/10.1017/S0016756801005313 Published online by Cambridge University Press

5.c. Ideal simple shear and pure shear

Because the sampling line is necessarily oblique to the Main Central Thrust, isograds inverted by ideal simple shear should always be associated with an inverted pressure field gradient, as both isograds and sampling line rotate toward the foreland during such a deformation (Fig. 6b). The lack of a clearly inverted pressure field gradient across the High Himalayan Crystalline Sequence of the Sutlej and other Himalayan sections (e.g. Hubbard, 1989; MacFarlane, 1995), consequently does not support an inversion of isograds through ideal simple shear only (Jain & Manickavasagam, 1993; Grujic *et al.* 1996; Hubbard, 1996; Grasemann & Vannay, 1999). The rotation of the sampling line toward the hinterland during ideal pure shear should result in peak pressures decreasing upwards across the exhumed metamorphic sequence. For such an ideal pure shear flow, isograds could be inverted by deformation only if the isotherms at peak were already steeper than the perpendicular to the Main Central Thrust (shortening eigenvector), in order to be located in the foreland-directed rotation sector of the strain ellipse (Fig. 6b). In any case, ideal pure shear could not account for the strong non-coaxial deformation observed in the rocks of the High Himalayan Crystalline Sequence (Fig. 3).

5.d. General shear

Combining simple shear and pure shear results in a general non-coaxial flow, characterized by a stretching eigenvector parallel to the shear zone boundaries, whereas the shortening eigenvector is oblique. The cosine of the angle between these irrotational directions corresponds to the 'kinematic vorticity number W_k', that is a measure of the relative amounts of simple shear and pure shear in the flow (Passchier, 1988; Passchier & Trouw, 1996; Fossen & Tikoff, 1997). In the case of a variable flow vorticity during progressive deformation, the flow is characterized by a 'mean kinematic vorticity number W_m', integrating the vorticity of the flow over space and time (Passchier, 1988). For naturally deformed rocks, W_m represents the mean value of the vorticity for the entire deformation history.

In contrast to ideal simple shear, material lines in a general shear flow can either co-rotate or counter-rotate with respect to the simple shear component of the flow. In order for the sampling line not to rotate and to remain parallel to the surface of the Earth during exhumation through a non-coaxial deformation, this line must be parallel to the horizontal shortening eigenvector of a general shear flow. Considering that the Main Central Thrust and High Himalayan Crystalline Sequence dip *c.* 30° to the northeast in the Sutlej section, ductile extrusion through a general shear flow characterized by a mean kinematic vorticity number $W_m \approx 0.86$ (= cosine 30°) reconciles non-coaxial deformation with the lack of significant pressure field gradient along the sampling line across the sequence (Fig. 6b). Furthermore, this lack of pressure field gradient is not compatible with a significantly heterogeneous deformation, and it indicates, consequently, a rather homogeneous shear flow at large scale. The *P–T* data for the Sutlej section indicate that isotherms at peak were oblique relative to the sampling line and dipping toward the foreland (if not already inverted). Consequently, the simple shear component of the flow must induce a co-rotation of the isograds (palaeoisotherms) toward the foreland during exhumation and cooling, eventually resulting in an inversion (Grasemann & Vannay, 1999). It should be noted that in a rock volume deforming by a homogeneous flow with a constant vorticity, all the samples record the same vorticity. Consequently, although the samples located along the shortening eigenvector of a general shear flow do not rotate one relative to another with respect to the shear zone boundaries, these samples are affected by the same relative amounts of simple shear and pure shear for a constant vorticity.

6. General shear extrusion kinematic model

On the basis of the previous considerations, a simple quantitative kinematic model illustrates how extrusion through a general non-coaxial flow could lead to inverted isograds consistent with the *P–T* field gradients measured across the High Himalayan Crystalline Sequence of the Sutlej section (Fig. 7). In this model, the metamorphic sequence is considered as a shear zone deforming ductilely by general shear between two rigid plates, as a consequence of underthrusting along the Main Central Thrust. The geometry of the model has been kept deliberately simple, so the relations between rotation and stretching of material lines can be easily assessed. The detachment at the top of the High Himalayan Crystalline Sequence is considered to represent a reactivation of the thrust beneath which the sequence was originally subducted (e.g. Dèzes *et al.* 1999; Vannay & Hodges, 1996). The dip and present-day thickness of the High Himalayan Crystalline Sequence, the maximum subduction depth of the sampling line, the mean kinematic vorticity number of the shear flow, and the large-scale homogeneous flow used in the model, are constrained by the results from the Sutlej section. Deformation is assumed to be isochoric plane strain flow. Post-Main Central Thrust external tilting of the shear zone with respect to the Earth's surface is neglected.

Because the model assumes deformation by general shear, the pure shear component of the flow induces a thinning of the metamorphic sequence that must be balanced by a perpendicular stretching of the unit parallel to its boundaries. As the unit has the geometry of a wedge closing at depth, its stretching is directed toward the surface, contributing to an extrusion of the

https://doi.org/10.1017/S0016756801005313 Published online by Cambridge University Press

metamorphic sequence. Because the metamorphic sequence is considered to be bounded by rigid plates, an extensional stretching fault (South Tibetan Detachment System) develops along the upper contact of the unit as a consequence of the extrusive flow (Means, 1989; Fossen & Tikoff, 1997). Similarly, the extrusive flow induces an overthrusting of the High Himalayan Crystalline Sequence toward the foreland along a basal stretching thrust fault, enhancing the slip rate along the Main Central Thrust relative to the underthrusting movement controlled by the overall plate convergence rate. Two parameters controlling the amount of extrusion are the finite thinning, and therefore the original thickness of the sequence, as well as the maximum subduction depth of this unit (Main Central Thrust–South Tibetan Detachment System convergence depth). The model presented in Figure 7 assumes that ductile extrusion ceases when the sampling line reaches the brittle–ductile transition depth around 15 km, after its exhumation from a 30 km depth. Because we still have no constraints on the finite strain in the High Himalayan Crystalline Sequence, its original thickness and maximum subduction depth have been assigned arbitrary, but realistic, values (17.5 and 50 km respectively in Fig. 7), in order for the sequence to be thinned to its present-day thickness of 10 km at the end of ductile extrusion.

7. Relevance and uncertainties of the model

The proposed model emphasizes how a general shear flow could reconcile inverted isograds with a lack of inverted pressure field gradient and a pervasive non-coaxial deformation. It is based, however, on several assumptions, and it ignores other processes potentially active during exhumation (e.g. dissipative thermal processes). Consequently, this simple geometric and kinematic model obviously represents only a first-order approximation for the possible tectono-metamorphic evolution during the exhumation of the High Himalayan Crystalline Sequence.

7.a. Homogeneity and vorticity of the flow

The large-scale, broadly homogeneous ductile flow illustrated in Figure 7 is not an unconstrained assumption of the model, as it is borne out by the lack of pressure field gradient across the studied metamorphic sequence (Figs 4, 6). From the Sutlej Valley area to the Garhwal Himalaya to the southeast, the High Himalayan Crystalline Sequence consists essentially of a fairly homogeneous sequence of metapelites and metapsammites, intercalated between a thick unit dominated by Proterozoic granite in its footwall, and a Cambro-Ordovician granitic pluton at the base of the Tethyan Himalaya in its hanging wall (Fig. 1). This lithotectonic setting is compatible with a ductile extrusion of the High Himalayan Crystalline Sequence by a general shear flow broadly homogeneous at large-scale. Such a large-scale homogeneous flow also implies strong strain gradients at the levels of both the Main Central Thrust and the detachment at the top of the unit, in good agreement with the presence of mylonitic zones along these contacts (Fig. 4). Moreover, such a strain distribution is also consistent with the finite strain pattern constrained across the High Himalayan Crystalline Sequence of the Garhwal and Kumaun regions, 50 and 230 km to the southeast of the studied area, respectively (Jain & Anand, 1988; Bhattacharya, 1999). These quantitative results indicate a fairly constant finite strain across most of the sequence, as well as clear gradients toward higher finite strain in the vicinity of the tectonic contacts of the unit.

It is also important to emphasize that a general shear extrusive flow does not even necessarily require the geometry of a wedge at the beginning of exhumation during Early Miocene times. Seismic data indicates that the Main Central Thrust and South Tibetan Detachment System converge at depth beneath the present-day surface. If these boundaries were parallel (or even diverging toward depth) at the onset of exhumation, then they must have converged at some later period. Such a large-scale convergence of these boundaries would imply significant induced pressure gradients along the shear zone (more pure shear at depth), and a heterogeneous general shear flow contributing to an extrusion, such as illustrated by the channel flow model of Grujic *et al.* (1996). Such a heterogeneous flow could not, however, be reconciled with the lack of pressure field gradient across the High Himalayan Crystalline Sequence of the Sutlej section.

In addition to the results of Grujic *et al.* (1996) for the Himalaya of Bhutan, a quantitative flow analysis of the Main Central Thrust zone in the Sutlej Valley confirms a deformation by general shear in the High Himalayan Crystalline Sequence, during at least part of its tectonic evolution. In these Main Central Thrust zone rocks, kinematic indicators indicate a shear flow with a vorticity $W_m \approx 0.57$–0.71 during a late stage of ductile deformation (Grasemann, Fritz & Vannay, 1999). In the High Himalayan Crystalline Sequence cropping out along the upper Sutlej section, C'-type shear bands, as well as abundant back-rotated asymmetric pull-aparts (boudinage), also indicate a general non-coaxial flow during ductile deformation (Passchier & Trouw, 1996; Grasemann & Stüwe, 2001). The meaning of quantitative kinematic indicators is certainly limited in space and time, since they possibly record only a part of the finite deformation, and the strain can be strongly partitioned at small-scale. The proposed model does not rely on such local kinematic measurements, but on the probable identification of a large-scale eigenvector, allowing an estimation of the mean kinematic vorticity number (Passchier, 1988), integrating the flow over space and time across the entire deforming rock volume.

https://doi.org/10.1017/S0016756801005313 Published online by Cambridge University Press

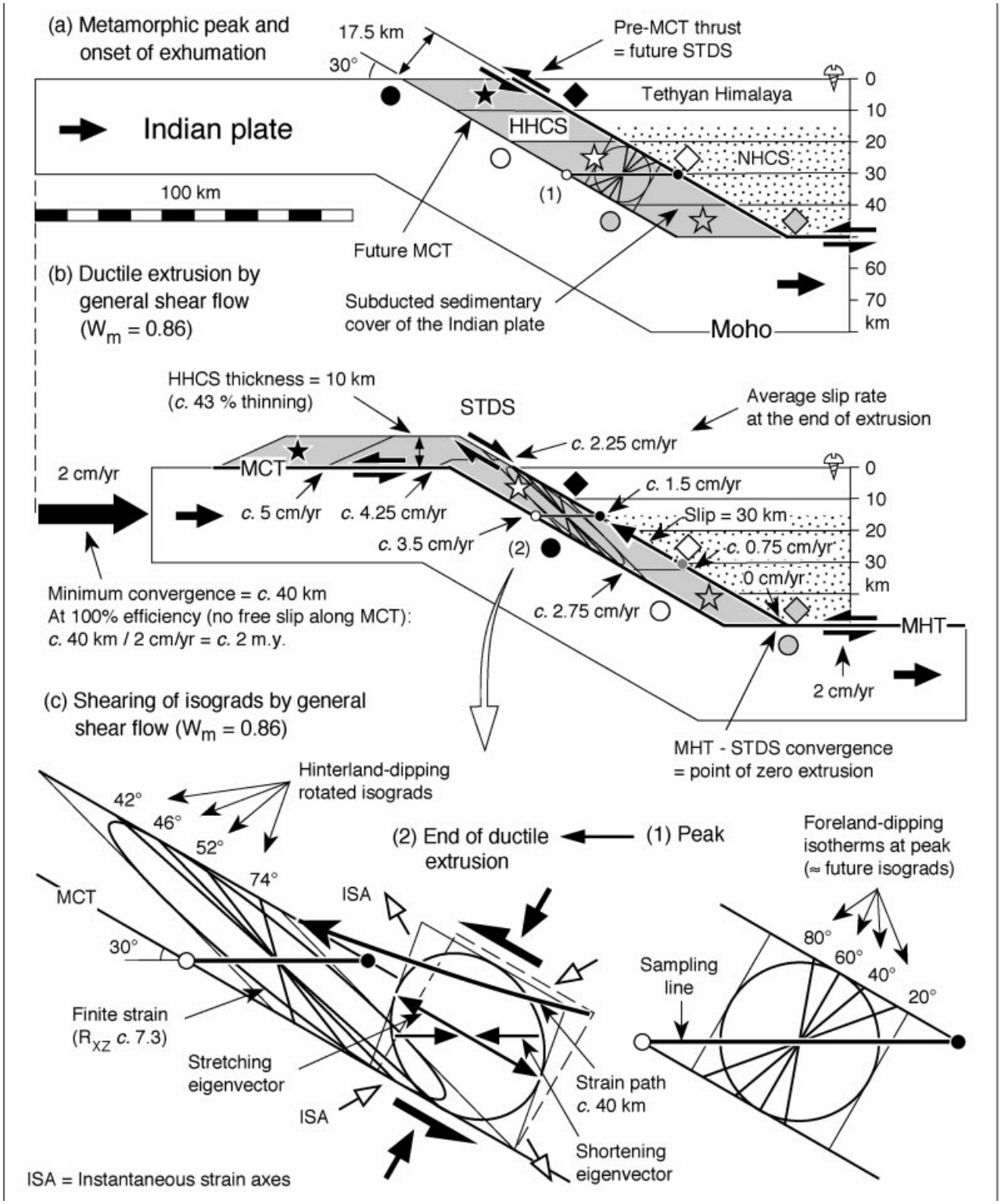


Figure 7. Kinematic model for an extrusion of the Himalayan crystalline core zone (HHCS) by a general non-coaxial flow. (a) Initial situation at metamorphic peak and onset of exhumation. The circles, stars and diamonds are undeforming markers. (b) Final situation at the end of ductile extrusion (abbreviations as in Figs 1 and 2). The model assumes that: (1) the High Himalayan Crystalline Sequence corresponds to a ductile shear zone delimited by two parallel boundaries (Main Central Thrust and South Tibetan Detachment System) dipping 30° to the northeast (present-day dip) and converging at depth; (2) the ductile extrusion occurs through a homogeneous, isochoric (constant volume), plane strain general flow; (3) the vorticity of the flow is W_m = 0.86 (= cos 30°) so the sampling line, that was parallel to the Earth's surface at peak (no pressure field gradient, Fig. 4), does not rotate during deformation (Fig. 6). The original thickness and the maximum subduction depth of the High Himalayan Crystalline Sequence (Main Central Thrust–South Tibetan Detachment System convergence depth) have been set in order for the unit to reach its present-day thickness of 10 km when the sampling line reaches the brittle–ductile transition depth (*c.* 15 km) during its extrusion from its maximum subduction depth of 30 km (Fig. 4). Assuming no decoupling (no 'free slip') at the level

https://doi.org/10.1017/S0016756801005313 Published online by Cambridge University Press

7.b. *P–T* constraints

The proposed model depends significantly on the *P–T* data showing a lack of clear peak pressure field gradient across the metamorphic sequence. The *P–T* results presented in Figure 4 have been constrained by four approaches: multiple equilibria thermobarometry, the predictions of a KFMASH petrogenetic grid for the stability of metapelitic assemblages, *P–T* path thermodynamic modelling, and oxygen isotope thermometry. Both the thermobarometry data and the petrogenetic grid have been calculated according to an internally consistent thermodynamic data base. The consistency between the *P–T* results obtained with various methods in each sample, as well as the consistency of these results from one sample to another across the entire sequence, is a strong argument that these data represent, within uncertainties, close estimates of peak conditions (Vannay, Sharp & Grasemann, 1999). Moreover, a detailed petrographic analysis of 90 samples from the Sutlej section indicate well-preserved peak assemblages (Vannay & Grasemann, 1998), and we are not aware of any non-tectonic process that could systematically buffer the depth-controlled pressure recorded by multiple equilibria across an entire metamorphic sequence. At larger-scale, numerous comparable thermobarometry results for the Himalaya indicate consistent *P–T* results for metapelites, from the garnet zone to partial melting (e.g. Dèzes *et al.* 1999), or even to eclogite facies conditions (e.g. Guillot *et al.* 1997). As will be discussed below, such results for the High Himalayan Crystalline Sequence generally indicate an upward decrease in peak pressure that is also compatible with a general shear extrusion.

It should also be noted that the concept illustrated in the proposed model does not depend on absolute pressure determinations, reflecting the absolute subduction depth of the samples, but on the lack of obvious difference in peak pressure across the High Himalayan Crystalline Sequence, indicating a constant depth at peak along the sampling line. Although the accuracy of thermobarometry is still limited, a precision better than ± 50 °C and ± 1 kbar can be routinely achieved when the same technique is used to determine differences in *P–T* conditions between samples (e.g. Worley & Powell, 2000). Given that the same methodology has been consistently applied to a suite of metapelitic assemblages well-suited for thermobarometry, the results obtained are consequently precise enough to confirm that there is no clear peak pressure field gradient across the High Himalayan Crystalline Sequence of the Sutlej section.

7.c. Thinning

A major limitation of the model is that the original thickness and maximum subduction depth of the High Himalayan Crystalline Sequence are not constrained and have been assigned arbitrary values (17.5 and 50 km, respectively, in Fig. 7). It is interesting to note, however, that the modelled extrusion is realistic if we consider the following points. (1) The present-day thickness of the High Himalayan Crystalline Sequence can reach up to 40 km in some sections (Jain & Manickavasagam, 1993; Searle *et al.* 1999*b*). (2) The Main Central Thrust–South Tibetan Detachment System convergence depth used in the model (50 km) is compatible with seismic data indicating that these structures apparently converge 30 to 40 km beneath the present-day surface at 90° E longitude (Fig. 2a, Hauck *et al.* 1998), as well as with the average 20 km of erosion of the High Himalayan range during the past 20 m.y. (Einsele, Ratschbacher & Wetzel, 1996). (3) The eclogites of the Tso Morari crystalline unit, 170 km to the north of the studied area, indicate that some metasedimentary rocks of the Indian plate have been subducted down to 70 km depth (20 kbar; Guillot *et al.* 1997). (4) For the modelled extrusion, the cartographic extent of the Main Central Thrust perpendicular to the range, from the basal sample to the foreland tip of the High Himalayan Crystalline Sequence (*c.* 100 km, Fig. 7b), is comparable to what is observed in several Himalayan sections (Figs 1, 2b; Brunel & Kienast, 1986; Pêcher, 1989). (5) The modelled extrusion induces an extensional movement of the sampling line, relative to the rocks of the Tethyan Himalaya, that compares well with quantitative estimates of minimum slip across some strands of the South Tibetan Detachment System (*c.* 30 km; Herren, 1987; Burchfiel *et al.* 1992; Dèzes *et al.* 1999). (6) The extrusion modelled in Figure 7 implies a thinning of the sequence by *c.* 43%. This value is comparable to thinning of other metamorphic sequences by up to 47% (Xypolias & Doutsos, 2000), or even 65% (Wallis, 1995), as constrained by quantitative vorticity and finite strain results.

of the Main Central Thrust (maximum efficiency), the minimum convergence required by the model, as constrained by the strain path (*c.* 40 km), is accommodated in *c.* 2 m.y. for an average convergence rate of 2 cm/yr. The average slip rates along the Main Central Thrust and South Tibetan Detachment System at the end of extrusion, as indicated for a 2 cm/yr convergence rate, increase linearly from the point of zero extrusion. (c) Enlarged diagrams illustrating the degree of rotation of isograds (≈ palaeoisotherms at peak) at the end of the general shear extrusion, as a function of the initial dip of the isotherms at peak (see text for discussion).

https://doi.org/10.1017/S0016756801005313 Published online by Cambridge University Press

7.d. Dip of the shear zone

The model illustrated in Figure 7 assumes a constant Main Central Thrust and High Himalayan Crystalline Sequence dip of 30°, similar to the present-day average value constrained by structural measurements (Fig. 3). The uncertainty in this dip angle, and therefore in the angle between the thrust and the sub-horizontal sampling line, propagates into an uncertainty in the mean kinematic vorticity number W_m. Changing the Main Central Thrust dip from 30° to 35° or 25° would modify W_m from 0.86 to 0.82 or 0.9, respectively, but this uncertainty does not affect the general concept of the model. An additional source of uncertainty is the potential influence of a post-Main Central Thrust tilting of the entire High Himalayan Crystalline Sequence, as a consequence of ongoing thrusting in the footwall of the unit. Geomagnetic results from the Himalaya of Nepal suggest that the High Himalayan Crystalline Sequence in the Everest–Makalu massif underwent a northward tilting of about 10° since Miocene times (Rochette *et al.* 1994). Assuming a similar tilting for this sequence of the Sutlej section implies that the present-day sub-horizontal sampling line also rotated northward by 10°, and that a sample at the base of the sequence was originally deeper than a sample at the top, relative to the Earth's surface. For a 10 km thick sequence, the basal sample should have been 3.5 km deeper than the top one before tilting, translating to a pressure difference of 0.9 kbar. Such a weak pressure field gradient across the High Himalayan Crystalline Sequence would remain compatible, within uncertainties, with the pressure data for the studied section (Fig. 4). The uncertainty on the original dip of the Main Central Thrust is therefore encompassed within the overall uncertainty of the model and it does not affect its plausibility.

8. General shear extrusion and syn-convergence extension

A major consequence of an extrusive flow in a metamorphic sequence is that it results in an extensional detachment along the upper contact of the unit (Fig. 7b). Such an extrusion-induced extension is consistent with the SW-directed non-coaxial deformation observed across most of the High Himalayan Crystalline Sequence, and with opposite NE-directed shearing restricted to the top of the unit (Fig. 3). Inasmuch as extrusion is the consequence of the wedge geometry of the metamorphic sequence and of its deformation controlled by the plate convergence, a general shear extrusion can reconcile kinematic extension with a compressional geodynamic setting.

8.a. South Tibetan Detachment System as a 'compressional extensional stretching fault'

In the model, the extrusive movement of the metamorphic rocks relative to the hanging wall of the South Tibetan Detachment System is a function of the finite thinning of the unit. Because the relative movement along the detachment decreases with depth to reach zero where the South Tibetan Detachment System and Main Central Thrust (or Main Himalayan Thrust) converge (Fig. 7b), a general shear extrusion can account for the paradoxical convergence of an extensional structure toward a major thrust, as indicated by seismic data (Fig. 2a; Hauck *et al.* 1998). Consequently, the model predicts that the South Tibetan Detachment System could be a stretching fault (Means, 1989; Fossen & Tikoff, 1997), recording an increasing displacement toward the surface of the Earth. As a function of the parameters controlling the amount of extrusion, and depending on the present-day structural level exposed by erosion, the model can also predict significant along-strike variations in the extensional slip along the detachment. This prediction is consistent with the fact that the South Tibetan Detachment System is not a continuous structure along the strike of the Himalayan orogen, in contrast to the Main Central Thrust that accommodated up to 250 km of shortening during the India–Asia convergence (e.g. Hodges, 2000). Moreover, the proposed general shear extrusion model predicts that the South Tibetan Detachment System is a direct consequence of the underthrusting of the Indian plate along the Main Central Thrust, accounting for the contemporaneousness of these structures.

A general shear extrusion of the Himalayan crystalline core zone implies that syn-convergence kinematic extension is compatible with dynamic compression, and that it does not necessarily reflect a minimum effective stress field (e.g. Burchfiel & Royden, 1985). This paradoxical situation emphasizes the need to clearly distinguish strain and stress (Marrett & Peacock, 1999). If the South Tibetan Detachment System is the consequence of a general shear extrusion, it must correspond to a stretching fault (Means, 1989). In order to emphasize its dynamics–kinematics causality, the South Tibetan Detachment System could consequently be described as a 'compressional extensional stretching fault'.

8.b. Timing

Geochronological and structural results indicate that the main extensional movement along some strands of the South Tibetan Detachment System occurred in a few million years or less, inducing a rapid exhumation of the High Himalayan Crystalline Sequence. In the Himalaya of Zanskar, an extensional slip of between 35 and 100 km occurred along the extensional Zanskar Shear Zone between approximately 23 and 20 Ma, implying an average slip rate between 1.2 and 3.3 cm/yr (Dèzes *et al.* 1999; Vance & Harris, 1999). For the Qomolangma Detachment in Nepal, an average slip rate as high as 4.7 cm/yr is calculated by Hodges *et al.* (1998). An additional challenge for the models proposing a mechanism for the Himalayan syn-

https://doi.org/10.1017/S0016756801005313 Published online by Cambridge University Press

convergence extension is to explain such a rapid movement. This question of timing is not quantitatively addressed in the models by Burchfiel & Royden (1985) and Grujic *et al.* (1996). As will be discussed below, the rapid, buoyancy-controlled exhumation simulated by the model of Chemenda *et al.* (1995) appears to be based on an unrealistically high Indo-Himalayan contraction rate.

The general shear extrusion model we propose can predict a rapid syn-convergence extension in a few million years, consistent with the available geophysical, structural and geochronological data. Because the general shear extrusion illustrated in Figure 7 is a direct consequence of the plate convergence, its timing is mainly controlled by two parameters: (1) the Indo-Himalayan convergence rate; and (2) the amount of the plate convergence movement that is transmitted along the Main Central Thrust into ductile deformation of the High Himalayan Crystalline Sequence. The efficiency of the extrusion process illustrated in Figure 7 depends consequently on the degree of ductile coupling between the footwall and hanging wall of the Main Central Thrust. At maximum efficiency, that is, allowing no 'free slip' along the Main Central Thrust, the minimum convergence movement must be equal to the strain path of the deformation induced in the overlying metamorphic sequence. For the simulated extrusion, the minimum convergence required is *c.* 40 km (Fig. 7c).

As reviewed by Hodges (2000), it is reasonable to speculate that one-third to one-half of the 1800–2750 km of convergence between the Indian plate and the stable Eurasia over the past 50 m.y. has been accommodated by contraction in the Himalaya itself. These estimates translate in an average contraction rate of 1.2–2.7 cm/yr, that compares well with estimates for recent to present-day periods. On the basis of various geological constraints, Powers, Lillie & Yeats (1998) calculated an average Indo-Himalayan convergence rate of 1.4 ± 0.4 cm/yr since Late Pliocene times. Present-day Global Positioning System measurements indicate that, out of the 5.8 ± 0.4 cm/yr convergence between India and Asia, an average contraction rate of 1.75 ± 0.2 cm/yr occurs across the Himalaya of Nepal (Bilham *et al.* 1997, and references therein). Assuming a rounded average convergence rate of 2 cm/yr, the general shear extrusion induced by the *c.* 40 km of plate convergence simulated in the model (Fig. 7) requires only *c.* 2 m.y. of underthrusting at maximum efficiency. Because it is a direct consequence of this convergence, the 30 km of ductile extension along the South Tibetan Detachment System, as simulated by the model, must take place during the same *c.* 2 m.y. time interval. As a consequence of this rapid extrusion, the average slip rate along the detachment increases from zero cm/yr at the Main Central Thrust–South Tibetan Detachment System convergence point, to reach 1.5 cm/yr at the level of the sampling line. Such a rapid slip rate is consistent with the available data (e.g. 1.2–3.3 cm/yr for the Zanskar Shear Zone: Dèzes *et al.* 1999). Because a general shear extrusion implies a tectonic movement accelerating toward the surface, it is also interesting to note that the slip rates at the surface could be underestimated by the measurements from present-day exposed structural levels.

It should kept in mind that the timing of the extrusion simulated in Figure 7 assumes maximum efficiency (no 'free slip' along the Main Central Thrust). Consequently, the calculated slip rates represent maximum values for the amount of extrusion modelled. If some 'free slip' occurs along the Main Central Thrust, the efficiency of the system is reduced, as only part of the plate convergence movement is transmitted into deformation of the hanging wall rocks. If only 50%, for example, of the underthrusting movement contributes to the simulated extrusion, twice as much underthrusting must occur along the Main Central Thrust (*c.* 80 km), and the process takes twice as long (*c.* 4 m.y.). It appears, nevertheless, that a general shear extrusion would remain a rapid geological process even at such a reduced efficiency. Moreover, a significant amount of 'free slip' between the underthrusting plate and the High Himalayan Crystalline Sequence during ductile deformation is not borne out by the continuous metamorphic and strain gradients generally observed across the Main Central Thrust in the internal parts of the orogen (e.g. Jain & Anand, 1988; Hubbard, 1989; Pêcher, 1989; Metcalfe, 1993). This lack of obvious decoupling along the thrust, beneath the brittle–ductile transition zone, implies that a high efficiency extrusive flow in the High Himalayan Crystalline Sequence is not unrealistic. Consequently, as a function of the amount of shearing the downgoing plate induces in its hanging wall, general shear extrusion could be a very efficient mechanism contributing to a rapid exhumation of high-grade metamorphic rocks.

9. Comparison with previous models for syn-convergence extension

The gravitational collapse model by Burchfiel & Royden (1985) is based on theoretical considerations about the distribution of stress in an orogen, whereas the buoyancy-controlled exhumation model by Chemenda *et al.* (1995) relies on the results of analogue simulations. Compared to these models, the quantitative general shear extrusion model we propose, as well as the qualitative channel flow extrusion model by Grujic *et al.* (1996), are more directly related to field and analytical constraints on strain, allowing determination of the actual kinematics associated with the development of natural structures during the Himalayan orogeny (e.g. Marrett & Peacock, 1999).

https://doi.org/10.1017/S0016756801005313 Published online by Cambridge University Press

9.a. General shear extrusion vs. buoyancy-controlled exhumation

The model by Chemenda *et al.* (1995) is compatible with an exhumation of the High Himalayan Crystalline Sequence associated with coeval movements along the Main Central Thrust and South Tibetan Detachment System, but the deep initial subduction depth of the Indian upper crust (*c.* 250 km) required by this model is not borne out by seismic data (Hauck *et al.* 1998). In contrast, a general shear extrusion does not require such a deep subduction, and it is therefore compatible with a shallow-dipping Moho beneath Himalaya and south Tibet (Fig. 2a). The analogue experiments by Chemenda *et al.* (1995) simulate a rapid buoyancy-controlled exhumation, compatible with the data (about 30 km of extension in 2 m.y.), for a simulated plate convergence rate of 5 cm/yr, but because these experiments assume an upper plate (Tibet) acting as a passive buttress, the convergence is accommodated essentially in the lower plate (Himalaya). As a consequence, the contraction rate across the simulated orogen (5 cm/yr) does not appear to be realistic, as it is about two to four times higher than the best estimates for the average Indo-Himalayan convergence rate since collision (1.2–2.7 cm/yr; e.g. Bilham *et al.* 1997; Powers, Lillie & Yeats, 1998; Hodges, 2000).

The new thermo-mechanical experiments by Chemenda, Burg & Mattauer (2000) indicate that, as function of the parameters controlling these analogue simulations, the buoyant upper crust can start to decouple from the sinking sub-crustal lithosphere at an early stage of the subduction, to become progressively underplated beneath the upper plate. These simulations do not show, however, the deep crustal subduction and subsequent buoyancy-controlled exhumation process observed in purely mechanical experiments (Chemenda *et al.* 1995). In contrast, the tectonic evolution of the Himalaya–Tibet system could have involved a large-scale underplating of the Indian upper crust beneath Tibet since Late Eocene times, in good agreement with seismic and tomographic results (Hauck *et al.* 1998; Van der Voo, Spakman & Bijwaard, 1999), and as suggested in a new geodynamic scenario by Chemenda, Burg & Mattauer (2000). In this latter interpretation, the High Himalayan Crystalline Sequence is considered as a crustal wedge exhuming through the combined effect of both Main Central Thrust and South Tibetan Detachment System between 22 and 15 Ma. Because this crustal wedge is described to be entirely bounded by other crustal units, buoyancy can no longer be invoked. Consequently, Chemenda, Burg & Mattauer (2000) proposed that both the High Himalayan Crystalline Sequence exhumation and the extension along the South Tibetan Detachment System were triggered by the erosion related to thrusting along the Main Central Thrust. Although erosion undoubtly contributed to the exhumation of the crystalline core zone of the Himalaya, this process cannot, by itself, explain a syn-convergence detachment reaching 15–30 km depth beneath the present-day surface (Hauck *et al.* 1996). Moreover, the average erosion rate for the Himalaya since Early Miocene times is about 1 mm/yr (e.g. Einsele, Ratschbacher & Wetzel, 1996) and it seems quite unlikely that erosion alone could explain a rapid syn-convergence extension related to a rock uplift of the High Himalayan Crystalline Sequence at an average rate *c.* 4–8 mm/yr (Dèzes *et al.* 1999; Hodges *et al.* 1998). However, by trapping a wedge of the subducted and metamorphosed sedimentary cover of the lower plate between two rheologically stronger granitic crusts, the crustal underplating observed in the new experiments by Chemenda, Burg & Mattauer (2000) could contribute to explain an overall geometric setting favourable to a ductile extrusion, such as illustrated in Figure 7.

9.b. Homogeneous general shear vs. heterogeneous channel flow extrusion

The metamorphic core of the Himalayan orogen corresponds mainly to a thick metasedimentary sequence, generally dominated by pelitic paragneiss (Fig. 1), although significant volumes of deformed Cambro-Ordovician granite, as well as thick series of calc-silicate gneiss, are also observed in various areas. Early Proterozoic granite gneiss in the footwall units of the Main Central Thrust could represent slices of the granitic basement of the Indian crust, but such rocks do not appear to be involved in the High Himalayan Crystalline Sequence itself (Fig. 1). The overall lithological composition, as well as a gradual transition observed between segments of the South Tibetan Detachment System, indicate that the High Himalayan Crystalline Sequence represents essentially a metamorphosed equivalent of the overlying, several kilometres thick, Proterozoic to Early Palaeozoic sedimentary series forming the base of the Tethyan Himalaya, and often intruded by *c.* 500 Ma granites (e.g. Gansser, 1964; Frank *et al.* 1973; Brunel & Kienast, 1986; Hubbard, 1989; Pêcher, 1989; Steck *et al.* 1993; MacFarlane, 1995; Vannay & Hodges, 1996; Searle *et al.* 1999*b*; Vannay & Grasemann, 1998; Dèzes *et al.* 1999; Wyss, Hermann & Steck, 1999). During the continental collision since Early Eocene times (55–50 Ma), these sediments were progressively subducted, and they underwent a prograde metamorphism above garnet grade since Early Oligocene times (*c.* 35 Ma: e.g. Vance & Harris, 1999). As a consequence of the general SW-directed propagation of the contractional deformation in the Indian plate margin, the creation of the Main Central Thrust around 23 Ma triggered the exhumation of these metamorphic rocks (e.g. Hodges, Parrish & Searle, 1996; Coleman, 1998). At the onset of this exhumation, most of the rocks of the High

https://doi.org/10.1017/S0016756801005313 Published online by Cambridge University Press

Himalayan Crystalline Sequence were at temperatures between 600 and 750 °C (e.g. Fig. 4). The low viscosity of such a sequence of hot and partially molten metamorphic rocks is obviously reflected by the ductile deformation observed in this unit all along the range (e.g. Fig. 3).

As discussed by Grujic *et al.* (1996), ductile extrusion could be approximated by a channel flow model, in which a viscous material is deformed between two non-parallel rigid sheets, as a consequence of two possible mechanisms: (1) shearing applied at the boundaries and inducing a uniform vorticity across the channel; and (2) lateral pressure gradients producing a pipe-flow effect, characterized by the highest velocities in the centre of the channel (Mancktelow, 1995). Grujic *et al.* (1996) proposed that the extrusion of the High Himalayan Crystalline Sequence in Bhutan was a hybrid between these processes, but with a dominant influence of the pipe-flow effect. Because the highest flow velocity in the centre of the channel implies a faster exhumation rate, such a flow should contribute to exhumation of deeper rocks in the centre of the channel relative to its lateral parts (e.g. fig. 9 in Grujic *et al.* 1996). Consequently, such a large-scale, heterogeneous channel flow should be reflected by the peak pressure profile across the exhumed metamorphic sequence, and a significant up-section pressure increase in the lower part of this unit should be observed. In contrast, the uniform pressure field gradient across the High Himalayan Crystalline Sequence in the Sutlej Valley (Fig. 4) indicates a broadly homogeneous shear flow, characterized by a constant mean kinematic vorticity number across most of the sequence (Fig. 6), and essentially induced by the underthrusting movement along the Main Central Thrust.

Although the lithological composition of the metamorphic sequence must strongly influence the degree of homogeneity vs. heterogeneity of the shear flow in this unit, it is important to remember that a general shear extrusion does not necessarily imply that the shear flow should be homogeneous (Grujic *et al.* 1996). As discussed above, the High Himalayan Crystalline Sequence can be lithologically heterogeneous in some areas and contain, notably, relatively large volumes of massive, pre-Tertiary granitic gneiss. In the Zanskar region, for example, 200 km to the northwest of the Sutlej Valley, the 40 km thick sequence is heterogeneous at a kilometric scale, and it contains thick domes and sheets of granitic gneiss intercalated by amphibolite facies to migmatitic paragneiss. This lithological and rheological heterogeneity is likely to induce localized pipe-flow effects at the kilometric scale, affecting the velocity profile of the ductile flow across the sequence. Such a heterogeneous shear flow implies differential exhumation rates across the High Himalayan Crystalline Sequence, as indeed suggested by the continuous heterogeneities observed in the detailed peak pressure and cooling age profiles determined by Searle *et al.* (1999*b*).

9.c. General shear extrusion vs. gravitational collapse

Although it can be induced by a ductile general shear flow at depth, exhumation in shallow structural levels, above the brittle–ductile transition zone, should be accommodated by more brittle deformation and erosion. Consequently, the surface expression of the South Tibetan Detachment System could reflect the tectonic collapse of the hanging wall of the extruding wedge, occurring episodically by brittle faulting. Such a strain regime is consistent with what is observed in the Alps (Maurer *et al.* 1997), where the seismic activity indicates that: (1) extensional faulting down to a maximum depth of 15 km occurs in the topographically high Penninic units, in the hanging wall of the Rhone–Simplon line; and (2) orogen-perpendicular contraction and orogen-parallel extension occur in the footwall of this tectonic line, in the Helvetic units. Maurer *et al.* (1997) interpret these results as indicative of a relative tectonic collapse of the Penninic Alps with respect to the exhuming Helvetic units. This kinematic interpretation does not imply, however, that such a relative collapse is necessarily controlled by topographic gradients and gravity (e.g. Burchfiel & Royden, 1985; Hodges, Parrish & Searle, 1996). Although the geodynamic context is not directly comparable to the Alps or the Himalaya, the fact that extensional faulting in the Andes is restricted to elevations above 3 km emphasizes the relatively limited influence of gravitational collapse in a collisional setting (Meijer, Govers & Wortel, 1997). Consequently, an alternative dynamic interpretation proposed by Maurer *et al.* (1997) for the contrasted kinematic regime observed in the Alps is that it could reflect an exhumation, possibly controlled by buoyancy forces (e.g. Chemenda *et al.* 1995), of the basement massifs located in the footwall of the Rhone–Simplon line (External Crystalline Massifs). It is also interesting to note that Dietrich & Casey (1989) proposed that the wedge-shaped, Helvetic sedimentary nappes, located between the granitic External Crystalline Massifs representing their basement and the Penninic crystalline nappes forming their hanging wall, were tectonically extruded by ductile general shear.

10. General shear extrusion and inverted isograds

The general shear extrusion model we propose suggests that inverted isograds in the High Himalayan Crystalline Sequence could reflect a sequence of both thermal and tectonic processes: (1) the thermal perturbation during continental subduction contributes to bend isotherms toward the foreland; and (2) ductile shearing by the simple shear component of the general non-coaxial flow contributes to a further rotation of the isograds

https://doi.org/10.1017/S0016756801005313 Published online by Cambridge University Press

(≈ palaeoisotherms) towards the foreland, during the subsequent exhumation and cooling. For the modelled extrusion, isotherms at peak (≈ future isograds) originally dipping toward the foreland at angles greater than 20° are inverted after deformation (Fig. 7c). For steeper original dips (60–80°), the finally inverted isograds would most likely appear as sub-parallel to the Main Central Thrust at cartographic scale (e.g. Pêcher, 1989). General shear extrusion can thus account for both ductile non-coaxial deformation and inverted isograds, without requiring inverted isotherms at peak.

Material lines in a general flow can either co-rotate or counter-rotate with respect to the simple shear component of the bulk shear flow, depending on their original orientation relative to the eigenvectors (Fig. 6b). Although the pressure data from the Sutlej section strongly suggest that the sampling line corresponds to the shortening eigenvector of the flow across the High Himalayan Crystalline Sequence, this should not necessarily be the case in all other Himalayan sections. For example, if the extrusion from the peak situation illustrated in Figure 7a occurred through a general shear with a vorticity lower than $W_m = 0.86$ (more pure shear), the shortening eigenvector would make an angle greater than 30° with respect to the stretching eigenvector, parallel to the Main Central Thrust, and it would consequently dip toward the foreland. In this case, a material line of constant depth at peak would be located in the counter-rotation sector of the strain ellipse (Fig. 6b), and it would therefore counter-rotate toward the hinterland during extrusion. As a consequence, the pressure measured along a horizontal sampling line across the exhumed unit would decrease upwards, although isograds could still be sheared and inverted if the isotherms at peak were dipping toward the foreland more steeply than the shortening eigenvector. Consequently, extrusion through general shear flow could also reconcile inverted isograds with an up-section decreasing pressure field gradient, as measured in several Himalayan sections (e.g. Brunel & Kienast, 1986; Hodges, LeFort & Pêcher, 1988; Hodges & Silverberg, 1988; Hubbard, 1989; Pêcher, 1989; MacFarlane, 1995; Rai *et al.* 1998; Fraser, Worley & Sandiford, 2000).

11. Comparison with previous models for inverted isograds

11.a. General shear vs. ideal simple shear rotation of isograds

Compared to the previous kinematic models invoking a ductile shearing of isograds in the High Himalayan Crystalline Sequence (Thöni, 1977; Jain & Manickavasagam, 1993; Grujic *et al.* 1996; Hubbard, 1996), the general shear extrusion model we propose shares the common prediction that the simple shear component of a ductile flow can contribute to an inversion of isograds. As analysed quantitatively by Grasemann & Vannay (1999), ideal simple shear is potentially the most efficient type of flow to rotate, and eventually invert, material lines such as isograds. This efficiency decreases with the vorticity, as the pure shear component increases, although, as discussed above (Fig. 6), such an ideal simple shear flow is not compatible with a constant, or even upward decreasing, peak pressure field gradient across the High Himalayan Crystalline Sequence. Additionally, ideal simple shear is not consistent with the available quantitative vorticity measurements for this metamorphic sequence (Grujic *et al.* 1996; Grasemann, Fritz & Vannay, 1999).

11.b. General shear extrusion and thermal evolution

Thermal models proposing that the inverted isograds in the High Himalayan Crystalline Sequence reflect syn-Main Central Thrust inverted isotherms (e.g. LeFort, 1975) do not appear to be compatible with a rapid exhumation of this unit, such as predicted by the proposed model (Fig. 7) and constrained by geochronological data (Hodges *et al.* 1998; Dèzes *et al.* 1999). During a general shear extrusion such as illustrated in Figure 7, the temperature evolution in the High Himalayan Crystalline Sequence is essentially controlled by the cooling effect of the upper and lower plates. The cooling effect of the upper plate is limited because, once subduction ceased, the thermal relaxation of the perturbed isotherms induces a temperature increase in the hanging wall of the underthrusted sequence (e.g. Fig. 5). This cooling effect is further hindered by the presence, in the upper plate, of the 10–15 km thick sedimentary series of the Tethyan Himalaya. Given their lower thermal conductivity compared to the underlying metamorphic rocks, these sediments are likely to act as a thermal barrier contributing to keeping the exhuming metamorphic rocks hot ('heat focussing': Jaupart & Provost, 1985). The cooling effect of the underthrusting Indian plate (Main Central Thrust footwall) is more significant because colder rocks from the surface of the Earth are continuously subducted against the rapidly exhuming metamorphic sequence. As a consequence, a rapid cooling of the Main Central Thrust hanging wall occurs, as constrained by several *P–T* paths (e.g. Hodges & Silverberg, 1988; Pêcher, 1989; Searle *et al.* 1999*b*). Such a rapid cooling makes it unlikely for the prograde metamorphic assemblages in the hanging wall of the Main Central Thrust to re-equilibrate during their retrograde evolution, in order to record potentially inverted isotherms.

Along-strike variations in the tectono-metamorphic evolution of the Himalaya, sometimes invoked to explain the variety of models proposed for its inverted metamorphism (e.g. Hubbard, 1989), appear to be correlated with along-strike variations in thickness. Where the High Himalayan Crystalline Sequence is thick (15–40 km), it is characterized by a clear evolution toward high-temperature/low-pressure conditions

https://doi.org/10.1017/S0016756801005313 Published online by Cambridge University Press

at its top (cordierite- and andalusite-bearing assemblages), as well as by an intense partial melting associated with large-scale granitic intrusions (e.g. Brunel & Kienast, 1986; Pêcher, 1989; Swapp & Hollister, 1991; MacFarlane, 1995; Dèzes *et al.* 1999; Searle *et al.* 1999*a*,*b*). Where this sequence is thinner (5–10 km), no clear evolution toward high-*T*/low-*P* conditions is observed, anatexis is less intense, and there are no large-scale granitic intrusions (e.g. Vannay & Hodges, 1996; Vannay & Grasemann, 1998). Such features can be explained by the differential cooling effect of both lower and upper plates on the extruding High Himalayan Crystalline Sequence, as a function of its thickness. For a thin extruding sequence, the cooling effect of the downgoing plate could affect the entire unit, hindering thermal relaxation. Consequently, high-*T*/low-*P* conditions could not be recorded because the rocks are continuously cooling during exhumation (e.g. Fig. 5). For a thick extruding sequence, the cooling effect of the lower plate will be less significant at the top of the exhuming unit. This reduced cooling, combined with the potential 'heat focussing' effect of the Tethyan Himalaya (Jaupart & Provost, 1985), could contribute to maintain high temperatures at the top of the extruding sequence, allowing these rocks to record high-*T*/low-*P* conditions, as well as enhanced decompression melting. Such an isothermal decompression is well constrained by several *P*–*T* paths for the top of thick sections across the High Himalayan Crystalline Sequence (e.g. Hodges & Silverberg, 1988; Pêcher, 1989; Dèzes *et al.* 1999; Searle *et al.* 1999*b*).

12. Conclusions

A general shear extrusion of the high-grade metamorphic rocks forming the crystalline core zone of the Himalayan orogen is consistent with: (1) the general lack of significantly inverted peak pressure field gradient across the High Himalayan Crystalline Sequence, despite the intense non-coaxial deformation systematically observed across this unit along the entire range; (2) kinematic indicators demonstrating a ductile deformation combining simple shear and pure shear in this metamorphic sequence (Grujic *et al.* 1996; Grasemann, Fritz & Vannay, 1999); (3) structural and *P*–*T* constraints indicating that the High Himalayan Crystalline Sequence, that corresponds essentially to the subducted sedimentary cover of the Indian plate, behaved as a low viscosity rock sequence during exhumation controlled by the Main Central Thrust, as a consequence of the previous high-grade metamorphism and partial melting at peak conditions between 600 and 750 °C (e.g. Gansser, 1964; Hodges, Parrish & Searle, 1996; Vannay & Hodges, 1996; Dèzes *et al.* 1999; Vannay, Sharp & Grasemann, 1999; Wyss, Hermann & Steck, 1999); and (4) seismic data indicating that the High Himalayan Crystalline Sequence has the geometry of a large-scale orogenic wedge bounded by the converging Main Central Thrust and South Tibetan Detachment System (Hauck *et al.* 1998), most likely as a consequence of the accretion of the sedimentary cover of the Indian crust during its underplating beneath Tibet (Chemenda, Burg & Mattauer, 2000).

Moreover, the general shear extrusion model we propose can predict: (1) inverted isograds in the High Himalayan Crystalline Sequence, as a consequence of a foreland-directed rotation of peak isograds induced by the simple shear component of the ductile flow; (2) a syn-orogenic extension compatible with a geodynamic compressional setting and reflected by a compressional extensional detachment; (3) a syn-orogenic extension coeval with underthrusting along the Main Central Thrust (e.g. Hubbard & Harrison, 1989; Hodges *et al.* 1992, 1998; Hodges, Parrish & Searle, 1996; Coleman, 1998; Dèzes *et al.* 1999), because this extension is a direct consequence of the deformation induced in the High Himalayan Crystalline Sequence by the subducting Indian plate; (4) a rapid syn-convergence extension in a few million years, as constrained by geochronological and structural data (Hodges *et al.* 1998; Dèzes *et al.* 1999); (5) a syn-convergence detachment converging at depth toward the Main Central Thrust–Main Himalayan Thrust (Hauck *et al.* 1998), because this detachment initiates at this convergence point as a stretching fault (Means, 1989) recording a gradually increasing slip toward the surface; and (6) a syn-convergence extension significantly variable along the strike of the orogen (e.g. Herren, 1987; Burchfiel *et al.* 1992; Hodges, Parrish & Searle, 1996; Coleman, 1998; Dèzes *et al.* 1999), as a function of the parameters controlling the amount of extrusion and the present-day structural level exposed.

The general shear extrusion model we propose does not claim to account in detail, and at all scales, for the complexity of a natural process like an orogeny. This simple geometric and kinematic model is, however, consistent with the geometry, lithological composition, kinematics, thermal evolution and timing of the Himalayan orogeny, and it appears to 'fit the numbers'. This overall consistency suggests that a general shear extrusive flow could be the first-order process controlling the exhumation and the related tectonothermal evolution of the metamorphic core of the Himalayan orogen.

A limited number of studies invoked ductile extrusion in other collisional settings. In the Swiss Alps, Dietrich & Casey (1989) developed a model of ductile extrusion by general non-coaxial flow to account for the wedge geometry of the Helvetic nappes, as well as for the metamorphic and strain gradients within these units. Additionally, a geometric–kinematic model by Escher & Beaumont (1997) suggests that a ductile extrusion, combining simple shear and wedge-shaped pure shear flow, could explain the creation and intrusion of high-pressure nappes in the Penninic Alps. In

https://doi.org/10.1017/S0016756801005313 Published online by Cambridge University Press

the Sanbagawa metamorphic belt of Japan, a quantitative vorticity and finite strain analysis demonstrates a clear general non-coaxial flow, as well as a thinning of 35 to 65% of the metamorphic sequence, suggesting that ductile extrusion could account for about half of the exhumation of these units from 30 to 15 km depth (Wallis, 1995). On the basis of comparable vorticity and finite strain results indicative of a general shear flow, and implying a thinning up to 47%, Xypolias & Doutsos (2000) recently proposed that ductile extrusion partly controlled nappe tectonics in the southwestern Hellenides. Together with the results of Grujic *et al.* (1996) for the Himalaya of Bhutan, and of the present contribution for the Northwest Himalaya, these studies suggest that the significance of general shear extrusion as an efficient mechanism for exhuming high-grade metamorphic rocks has been underestimated (e.g. Platt, 1993). This conclusion could and should be assessed by a quantitative approach of ductile deformation in high-grade metamorphic sequences, aiming at constraining the vorticity of the ductile flow.

Acknowledgements. We thank Mary Hubbard and Jean-Pierre Burg for critical reviews that helped us to clarify several of our arguments, further test the proposed model, and discover some of its unexplored predictions. We thank Mike Cosca, Pierre Dèzes, Arthur Escher, Neil Mancktelow and Albrecht Steck for internal reviews and fruitful discussions. Jean-Claude Vannay and Bernhard Grasemann acknowledge support from the 'Swiss National Science Foundation' (FNRS grants 20-45063.95 and 20-52165.97, director A. Steck) and from the 'Austrian Science Fund' (FWF grants P-14129-GEO and P-13227-GEO).

References

Bhattacharya, A. R. 1999. Deformational regimes across the Kumaun Himalaya: a study in strain patterns. In *Geodynamics of the NW Himalaya* (eds A. K. Jain and R. M. Manickavasagam), pp. 81–90. Gondwana Research Group Memoir no. 6, Japan.

Bilham, R., Larson, K., Freymueller, J. & Project Idylhim members. 1997. GPS measurements of present-day convergence across the Nepal Himalaya. *Nature* **386**, 61–4.

Brunel, M. & Kienast, J.-R. 1986. Etude pétro-structurale des chevauchements ductiles himalayens sur la transversale de l'Everest-Makalu (Népal oriental). *Canadian Journal of Earth Science* **23**, 1117–37.

Burchfiel, B. C., Chen, Z., Hodges, K. V., Liu, Y., Royden, L. H., Deng, C. & Xu, J. 1992. The South Tibetan detachment system, Himalayan Orogen; extension contemporaneous with and parallel to shortening in a collisional mountain belt. *Geological Society of America Special Papers* **269**, 41 pp.

Burchfiel, B. C. & Royden, L. H. 1985. North–south extension within the convergent Himalayan region. *Geology* **13**, 679–82.

Burg, J. P., Brunel, M., Gapais, D., Chen, G. M. & Liu, G. H. 1984. Deformation of leucogranites of the crystalline main central thrust sheet in southern Tibet (China). *Journal of Structural Geology* **6**, 535–42.

Catlos, E. J., Harrison, T. M., Searle, M. P. & Hubbard, M. S. 1999. Evidence for late Miocene reactivation of the Main Central Thrust: from Garhwal to the Nepali Himalaya. *Terra Nostra* **99**, 20–2.

Chemenda, A. I., Burg, J.-P. & Mattauer, M. 2000. Evolutionary model of the Himalaya–Tibet system: geopoem based on new modelling, geological and geophysical data. *Earth and Planetary Science Letters* **174**, 397–409.

Chemenda, A. I., Mattauer, M., Malavieille, J. & Bokun, A. N. 1995. A mechanism for syn-collisional rock exhumation and associated faulting: Results from physical modelling. *Earth and Planetary Science Letters* **132**, 225–32.

Coleman, M. E. 1998. U–Pb constraints on Oligocene–Miocene deformation and anatexis within the Central Himalaya, Marsyandi valley, Nepal. *American Journal of Science* **298**, 553–71.

Dèzes, P. J., Vannay, J.-C., Steck, A., Bussy, F. & Cosca, M. 1999. Synorogenic extension; quantitative constraints on the age and displacement of the Zanskar Shear Zone (northwest Himalaya). *Geological Society of America Bulletin* **111**, 364–74.

Dietrich, D. & Casey, M. 1989. A new tectonic model for the Helvetic nappes. In *Alpine Tectonics* (eds M. P. Coward, D. Dietrich and R. G. Park), pp. 47–63. Geological Society of London, Special Publication no. 45.

Edwards, M. A. & Harrison, T. M. 1997. When did the roof collapse? Late Miocene north–south extension in the high Himalaya revealed by Th–Pb monazite dating of the Khula Kangri granite. *Geology* **25**(6), 543–6.

Einsele, G., Ratschbacher, L. & Wetzel, A. 1996. The Himalaya–Bengal Fan denudation–accumulation system during the past 20 Ma. *Journal of Geology* **104**, 163–84.

England, P. & Molnar, P. 1993. The interpretation of inverted metamorphic isograds using simple physical calculations. *Tectonics* **12**, 145–57.

England, P. C. & Thompson, A. B. 1984. Pressure–temperature–time paths of regional metamorphism I. Heat transfer during the evolution of regions of thickened continental crust. *Journal of Petrology* **25**, 894–928.

Ernst, W. G. & Peacock, S. M. 1996. A thermotectonic model for preservation of ultrahigh-pressure phases in metamorphosed continental crust. In *Subduction top to bottom* (eds G. E. Bebout, D. W. Scholl, S. H. Kirby and J. P. Platt), pp. 171–8. Geophysical Monograph no. 96. Washington: American Geophysical Union.

Escher, A. & Beaumont, C. 1997. Formation, burial and exhumation of basement nappes at crustal scale: a geometric model based on the Western Swiss-Italian Alps. *Journal of Structural Geology* **19**, 955–74.

Fielding, E. 1996. Tibet uplift and erosion. *Tectonophysics* **260**, 55–84.

Fossen, H. & Tikoff, B. 1997. Forward modeling of non-steady-state deformations and the "minimum strain path". *Journal of Structural Geology* **19**, 987–96.

Frank, W., Hoinkes, G., Miller, C., Purtscheller, F., Richter, W. & Thoeni, M. 1973. Relations between metamorphism and orogeny in a typical section of the Indian Himalayas; NW-Himalaya; S-Lahul, Kulu; Himachal Pradesh; first comprehensive report. *Tschermaks Mineralogische Petrographische Mitteilungen* **20**, 303–32.

Fraser, G., Worley, B. & Sandiford, M. 2000. High-precision geothermobarometry across the High Himalayan

https://doi.org/10.1017/S0016756801005313 Published online by Cambridge University Press

metamorphic sequence, Langtang Valley, Nepal. *Journal of Metamorphic Geology* **18**, 665–81.

Gansser, A. 1964. *Geology of the Himalayas*. London: Wiley Interscience, 289 pp.

Grasemann, B. 1993. Numerical modelling of the thermal history of the NW Himalayas, Kullu Valley, India. In *Himalayan Tectonics* (eds P. J. Treloar and M. P. Searle), pp. 475–84. Geological Society of London, Special Publication no. 74.

Grasemann, B., Fritz, H. & Vannay, J.-C. 1999. Quantitative kinematic flow analysis from the Main Central Thrust Zone (NW-Himalaya, India): implications for a decelerating strain path and the extrusion of orogenic wedges. *Journal of Structural Geology* **21**, 837–53.

Grasemann, B., Ratschbacher, L. & Hacker, B. R. 1998. Exhumation of ultrahigh-pressure rocks: thermal boundary conditions and cooling history. In *When continents collide: geodynamics and geochemistry of ultrahigh-pressure rocks* (eds B. R. Hacker and J. G. Liou), pp. 117–39. The Netherlands: Kluwer Academic Publishers.

Grasemann, B. & Stüwe, K. 2001. The development of flanking folds during simple shear and their use as kinematic indicators. *Journal of Structural Geology* **23**, 715–24.

Grasemann, B. & Vannay, J.-C. 1999. Flow controlled inverted metamorphism in shear zones. *Journal of Structural Geology* **21**, 743–50.

Grujic, D., Casey, M., Davidson, C., Hollister, L. S., Kündig, R., Pavlis, T. & Schmid, S. 1996. Ductile extrusion of the Higher Himalayan Crystalline in Bhutan: evidence from quartz microfabrics. *Tectonophysics* **260**, 21–43.

Guillot, S., De Sigoyer, J., Lardeaux, J. M. & Mascle, G. 1997. Eclogitic metasediments from the Tso Morari area (Ladakh, Himalaya): evidence for continental subduction during India-Asia convergence. *Contributions to Mineralogy and Petrology* **128**, 197–212.

Harrison, T. M., Grove, M., Lovera, M. & Catlos, E. J. 1998. A model for the origin of Himalayan anatexis and inverted metamorphism. *Journal of Geophysical Research* **103**, 27017–32.

Hauck, M. L., Nelson, K. D., Brown, L. D., Zhao, W. & Ross, A. R. 1998. Crustal structure of the Himalayan orogen at 90° east longitude from Project INDEPTH deep reflection profiles. *Tectonics* **17**, 481–500.

Herren, E. 1987. Zanskar shear zone; northeast–southwest extension within the Higher Himalayas (Ladakh, India). *Geology* **15**, 409–13.

Hodges, K. V. 2000. Tectonics of the Himalaya and southern Tibet from two perspectives. *Geological Society of America Bulletin* **112**, 324–50.

Hodges, K. V., Bowring, S., Davidek, K., Hawkins, D. & Krol, M. 1998. Evidence for rapid displacement on Himalayan normal faults and the importance of tectonic denudation in the evolution of mountain ranges. *Geology* **26**, 481–576.

Hodges, K. V., LeFort, P. & Pêcher, A. 1988. Possible thermal buffering by crustal anatexis in collisional orogens: thermobarometric evidence from the Nepalese Himalaya. *Geology* **16**, 707–10.

Hodges, K. V., Parrish, R. R., Housh, T. B., Lux, D. R., Burchfiel, B. C., Royden, L. H. & Chen, Z. 1992. Simultaneous Miocene extension and shortening in the Himalayan Orogen. *Science* **258**, 1466–9.

Hodges, K. V., Parrish, R. R. & Searle, M. P. 1996. Tectonic evolution of the central Annapurna Range, Nepalese Himalayas. *Tectonics* **15**, 1264–91.

Hodges, K. V. & Silverberg, D. S. 1988. Thermal evolution of the Greater Himalaya, Garhwal, India. *Tectonics* **7**, 583–600.

Holland, T. J. B. & Powell, R. 1998. An internally consistent thermodynamic data set for phases of petrological interest. *Journal of Metamorphic Geology* **16**, 309–43.

Hubbard, M. S. 1989. Thermobarometric constraints on the thermal history of the Main Central Thrust Zone and Tibetan Slab, eastern Nepal Himalaya. *Journal of Metamorphic Geology* **7**, 19–30.

Hubbard, M. S. 1996. Ductile shear as a cause of inverted metamorphism: Example from the Nepal Himalaya. *Journal of Geology* **104**, 493–9.

Hubbard, M. S. & Harrison, T. M. 1989. $^{40}Ar/^{39}Ar$ age constraints on deformation and metamorphism in the Main Central Thrust Zone and Tibetan Slab, eastern Nepal Himalaya. *Tectonics* **8**, 865–80.

Huerta, A. D., Royden, L. H. & Hodges, K. V. 1996. The interdependence of deformation and thermal processes in mountain belts. *Science* **273**, 637–9.

Jain, A. K. & Anand, A. 1988. Deformation and strain patterns of an intracontinental collision ductile shear zone – an example from the Higher Garhwal Himalaya. *Journal of Structural Geology* **10**, 717–34.

Jain, A. K., Kumar, D., Singh, S., Kumar, A. & Lal, N. 2000. Timing, quantification and tectonic modelling of Pliocene–Quaternary movements in the NW Himalaya: evidence from fission track dating. *Earth and Planetary Science Letters* **179**, 437–51.

Jain, A. K. & Manickavasagam, R. M. 1993. Inverted metamorphism in the intracontinental ductile shear zone during Himalayan collision tectonics. *Geology* **21**, 407–10.

Jamieson, R. A., Beaumont, C., Hamilton, J. & Fullsack, P. 1996. Tectonic assembly of inverted metamorphic sequences. *Geology* **24**, 839–42.

Jaupart, C. & Provost, A. 1985. Heat focussing, granite genesis and inverted metamorphic gradients in continental collision zones. *Earth and Planetary Science Letters* **73**, 385–97.

Kayal, J. R. 1996. Precursor seismicity, foreshocks and aftershocks of the Uttarkashi earthquake of October 20, 1991 at Garhwal Himalaya. *Tectonophysics* **263**, 339–45.

LeFort, P. 1975. Himalayas: the collided range. Present knowledge of the continental arc. *American Journal of Science* **275**, 1–44.

MacFarlane, A. M. 1995. An evaluation of the inverted metamorphic gradient at Langtang National Park, central Nepal Himalaya. *Journal of Metamorphic Geology* **13**, 595–612.

Mallet, F. R. 1875. On the geology and mineral resources of the Darjiling district and the western Duars. *Memoirs of the Geological Survey of India* **11**, 1–50.

Mancktelow, N. S. 1995. Nonlithostatic pressure during sediment subduction and the development and exhumation of high pressure metamorphic rocks. *Journal of Geophysical Research* **100**, 571–83.

Marrett, R. & Peacock, D. C. P. 1999. Strain and stress. *Journal of Structural Geology* **21**, 1057–63.

Maurer, H. R., Burkhard, M., Deichmann, N. & Green, A. G. 1997. Active tectonism in the central Alps: contrasting stress regimes north and south of the Rhone Valley. *Terra Nova* **9**, 91–4.

https://doi.org/10.1017/S0016756801005313 Published online by Cambridge University Press

MEANS, W. D. 1989. Stretching faults. *Geology* **17**, 893–6.
MEIJER, P. TH., GOVERS, R. & WORTEL, M. J. R. 1997. Forces controlling the present-day state of stress in the Andes. *Earth and Planetary Science Letters* **148**, 157–70.
METCALFE, R. P. 1993. Pressure, temperature and time constraints on metamorphism across the Main Central Thrust zone and High Himalayan Slab in the Garhwal Himalaya. In *Himalayan Tectonics* (eds P. J. Treloar and M. P. Searle), pp. 485–509. Geological Society of London, Special Publication no. 74.
MOLNAR, P. & LYON-CAEN, H. 1989. Fault plane solutions of earthquakes and active tectonics of the Tibetan Plateau and its margins. *Geophysical Journal International* **99**, 123–53.
NAJMAN, J. & GARZANTI, E. 2000. Reconstructing early Himalayan tectonic evolution and paleogeography from Tertiary foreland basin sedimentary rocks, northern India. *Geological Society of America Bulletin* **112**, 435–49.
NI, J. & BARAZANGI, M. 1984. Seismotectonics of the Himalayan collision zone: geometry of the underthrusting Indian plate beneath the Himalaya. *Journal of Geophysical Research* **89**, 1147–63.
PASSCHIER, C. W. 1988. The use of Mohr circles to describe non-coaxial progressive deformation. *Tectonophysics* **149**, 323–38.
PASSCHIER, C. W. & TROUW, R. A. J. 1996. *Microtectonics*. Berlin: Springer Verlag, 289 pp.
PÊCHER, A., 1989. The metamorphism in the central Himalaya. *Journal of Metamorphic Geology* **7**, 31–41.
PLATT, J. P. 1993. Exhumation of high-pressure rocks: a review of concepts and processes. *Terra Nova* **5**, 119–33.
POWELL, R. & HOLLAND, T. 1994. Optimal geothermometry and geobarometry. *American Mineralogist* **79**, 120–33.
POWERS, P. M., LILLIE, R. J. & YEATS, R. S. 1998. Structure and shortening of the Kangra and Dehra Dun reentrants, Sub-Himalaya, India. *Geological Society of America Bulletin* **110**, 1010–27.
PRINCE, C., VANCE, D., HARRIS, N. B. W. & OBERLI, F. 1994. Controls on and timing of metamorphism in the Himalaya. *Mineralogical Magazine* **62A**, 1210–11.
RAI, S. M., GUILLOT, S., LEFORT, P. & UPRETI, B. N. 1998. Pressure–temperature evolution in the Kathmandu and Gosaikund regions, Central Nepal. *Journal of Asian Earth Sciences* **16**, 283–98.
RAMBERG, H. 1975. Particle paths, displacement and progressive strain applicable to rocks. *Tectonophysics* **28**, 1–37.
ROCHETTE, P., SCAILLET, B., GUILLOT, S., LEFORT, P. & PÊCHER, A. 1994. Magnetic properties of the High Himalayan leucogranites: structural implications. *Earth and Planetary Science Letters* **126**, 1217–34.
ROYDEN, L. H. 1993. The steady state thermal structure of eroding orogenic belts and accretionary prisms. *Journal of Geophysical Research* **98**, 4487–507.
SEARLE, M. P., NOBLE, S. R., HURFORD, A. J. & REX, D. C. 1999*a*. Age of crustal melting, emplacement and exhumation history of the Shivling leucogranite, Garhwal Himalaya. *Geological Magazine* **136**, 513–25.
SEARLE, M. P., WATERS, D. J., DRANSFIELD, M. W., STEPHENSON, B. J., WALKER, C. B., WALKER, J. D. & REX, A. J. 1999*b*. Thermal and mechanical models for the structural and metamorphic evolution of the Zanskar High Himalaya. In *Continental tectonics* (eds C. Mac Niocaill and P. D. Ryan), pp. 139–56. Geological Society of London, Special Publication no. 164.
SHI, Y. & WANG, C. H. 1987. Two dimensional modelling of the *P–T–t* path of regional metamorphism in simple overthrust terrains. *Geology* **15**, 1048–51.
SORKHABI, R. B., STUMP, E., FOLAND, K. A. & JAIN, A. K. 1996. Fission-track and $^{40}Ar/^{39}Ar$ evidence for episodic denudation of the Gangotri granites in the Garhwal Higher Himalaya, India. *Tectonophysics* **260**, 187–99.
STECK, A., SPRING, L., VANNAY, J.-C., MASSON, H., BUCHER, H., STUTZ, E., MARCHANT, R. & TIÈCHE, J.-C. 1993. The tectonic evolution of the Northwestern Himalaya in eastern Ladakh and Lahul, India. In *Himalayan Tectonics* (eds P. J. Treloar and M. P. Searle), pp. 265–76. Geological Society of London, Special Publication no. 74.
SWAPP, S. M. & HOLLISTER, L. S. 1991. Inverted metamorphism within the Tibetan Slab of Bhutan: evidence for a tectonically transported heat-source. *Canadian Mineralogist* **29**, 1019–41.
THÖNI, M. 1977. Geology, structural evolution and metamorphic zoning in the Kulu Valley (Himachal Himalayas, India) with special reference to the reversed metamorphism. *Mitteilung der Gesellschaft der Geologie und Bergbaustudenten in Osterreichs* **24**, 125–87.
TRELOAR, P. J., BROUGHTON, R. D., WILLIAMS, M. P., COWARD, M. P. & WINDLEY, B. F. 1989. Deformation, metamorphism and imbrication of the Indian plate, south of the Main Mantle Thrust, north Pakistan. *Journal of Metamorphic Geology* **7**, 111–25.
VAN DER VOO, R., SPAKMAN, W. & BIJWAARD, H. 1999. Tethyan subducted slabs under India. *Earth and Planetary Science Letters* **171**, 7–20.
VANCE, D. & HARRIS, N. 1999. Timing of prograde metamorphism in the Zanskar Himalaya. *Geology* **27**, 395–8.
VANNAY, J.-C. & GRASEMANN, B. 1998. Inverted metamorphism in the High Himalaya of Himachal Pradesh (NW India): phase equilibria versus thermobarometry. *Schweizerische Mineralogische und Petrographische Mitteilungen* **78**, 109–35.
VANNAY, J. C. & HODGES, K. V. 1996. Tectonometamorphic evolution of the Himalayan metamorphic core between the Annapurna and Dhaulagiri, central Nepal. *Journal of Metamorphic Geology* **14**, 635–56.
VANNAY, J.-C., SHARP, Z. D. & GRASEMANN, B. 1999. Himalayan inverted metamorphism constrained by oxygen isotope thermometry. *Contributions to Mineralogy and Petrology* **137**, 90–101.
WALLIS, S. 1995. Vorticity analysis and recognition of ductile extension in the Sanbagawa belt, SW Japan. *Journal of Structural Geology* **8**, 1077–93.
WORLEY, B. & POWELL, R. 2000. High-precision thermobarometry: theory and a worked example. *Journal of Metamorphic Geology* **18**, 91–101.
WYSS, M., HERMANN, J. & STECK, A. 1999. Structural and metamorphic evolution of the northern Himachal Himalaya, NW India (Spiti-eastern Lahul-Parvati valley traverse). *Eclogae geologicae Helvetiae* **92**, 3–44.
XYPOLIAS, P. & DOUTSOS, T. 2000. Kinematics of rock flow in a crustal-scale shear zone: implication for the orogenic evolution of the southwestern Hellenides. *Geological Magazine* **137**, 81–96.

https://doi.org/10.1017/S0016756801005313 Published online by Cambridge University Press